CHAPTER 9:
References

In This Chapter...

9.1 References

- Bessell, M. S. (1990), *UBVRI Passbands*, P.A.S.P. 102, 1181.
- Biretta, J. A, and Sparks, W. B. (1995), *WFPC2 Polarization Observations: Strategies, Apertures, and Calibration Plans*, WFPC2 ISR 95-01.
- Biretta, J. A., (1995) "WFPC2 Flat Field Calibration," in *Calibrating Hubble Space Telescope: Post Servicing Mission*, eds. A. Koratkar and C. Leitherer, p. 257.
- Blouke, D. P., (1991), eds. Janesick, J. and Elliot, T., in P.A.S.P., 8, 153.
- Burrows, C. et al., (1991) *The Imaging Performance of the Hubble Space Telescope*, Ap. J. Lett. 369, L21.
- Clarke, J.T. and the WFPC2 IDT (1992), "White Paper for WFPC2 Far-Ultraviolet Science."[1]
- *Dithering: Relationship Between POS TARG's and CCD Rows/Columns.*[1]
- Evans, R. E. 1992, JPL Memorandum, DFM #2031.
- Gilliland, R. L., (1994) Ap.J. 435, L63.
- Groth, E. and Shaya, E., (1991), in *Wide Field/Planetary Camera Final Orbital/Science Verification Report*, S., M., Faber, Ed.
- Griffiths, R. Ewald, S. and MacKenty, J. W., (1989) in *CCDs in Astronomy*, P.A.S.P. 8, 231, ed. G. Jacoby.
- Gunn, J. E., and Oke, J. B. (1983), Ap.J. 266, 713.
- Harris, H. C., et al., (1991) *Photometric Calibration of the HST WF/PC-1 Camera: I. Ground Based Observations of Standard Stars*, A.J. 101, 677.

1. These documents may be requested by e-mail from `help@stsci.edu`.

- *HST Data Handbook*, C. Leitherer, ed., (Version 2.0, December 1995).[1]
- *HST Phase 2 Proposal Instruction*, (Version 8.0, 15 December 1995).[1]
- Hasan, H. and Bely, P., (1993) *Restoration of HST Images and Spectra II,* p.157.
- Hasan, H. and Burrows, C. J., (1993) "Calibrations of the Hubble Space Telescope Optical Telescope Assembly" in *Calibrating Hubble Space Telescope,* eds. C. Blades and S. Osmer, p. 395.
- Harris, et al., (1991) A.J. 101, 677.
- Holtzman, J., et al., (1995a), *The Performance and Calibration of WFPC2 on the Hubble Space Telescope*, P.A.S.P., 107, 156.
- Holtzman, J., et al., (1995b), *The Photometric Performance and Calibration of WFPC,* P.A.S.P., 107, 1065.
- Interface Control Document (ICD) 19, "PODPS to STSDAS".
- Interface Control Document (ICD) 47, "PODPS to CDBS".
- Janesick, J., Elliot, T., Bredthauer, R., Cover, J., Schaefer, R. and Varian, R., (1989) in *Optical Sensors and Electronic Photography*, SPIE Proc. 1071.
- Janesick, J., Elliot, T., Blouke, M. and Corrie, B., (1989b), in *Optical Sensors and Electronic Photography*, SPIE Proc. 1071, 115, ed. B. Pophal.
- Jordan, Deltorn, and Oates, (1993) *Greenwich Observatory Newsletter*, Sept. 1993.
- Koornneef, J. et al., (1983) "Synthetic Photometry and the Calibration of the Hubble Space Telescope," in *Highlights of Astronomy*, 7, 833, ed. J.-P. Swings.
- Krist, J. and Burrows, C., (1995) *Applied Optics*.
- Krist, J. E., (1995) "WFPC2 Ghosts, Scatter, and PSF Field Dependence," in *Calibrating Hubble Space Telescope: Post Servicing Mission*, eds. A. Koratkar and C. Leitherer, p. 311.
- Lauer, T. (1989), *The Reduction of WF/PC Camera Images*, P.A.S.P. 101, 445.
- Lauer, T., (1991) in *Wide Field/Planetary Camera Final Orbital/Science Verification Report*, ed. S. M. Faber.
- Oke, J.B. and Gunn, J., (1983), Ap.J. 266, 713.
- *STSDAS Calibration Guide* (November 1991).[1]
- STDAS Users' Guide.
- Schneider, D. P., Gunn, J. E., and Hoessel, J. G. (1983), Ap.J. 264, 337.
- Trauger, J. T., (1989), in *CCDs in Astronomy*, P.A.S.P. 8, 217, ed. G. Jacoby.
- Trauger, J. T., ed., (1993). *The WFPC2 Science Calibration Report*, Pre-launch Version 1.2. [IDT calibration report]

- WF/PC-1 IDT OV/SV Report.
- WFPC2 World Wide Web page at address: `http://www.stsci.edu/ftp/instrument_news/WFPC2/wfpc2_top.html`
- Westphal, J., et al. (1982), *The Wide Field/Planetary Camera in The Space Telescope Observatory*, IAU 18th General Assembly, Patras, NASA CP-2244.
- Woodgate, B. E., (1989) in *CCDs in Astronomy*, P.A.S.P. 8, 237, ed. G. Jacoby.

9.2 Instrument Science Reports[2]

- 96-02: Baggett, et al., *Contamination Correction in SYNPHOT for WFPC2 and WF/PC-1.*
- 96-01: Stiavelli and Baggett, 01/96, *Internal Flat Field Monitoring.*
- 95-07: Baggett, Casertano, and Biretta, 12/95, *WFPC2 Cycle 4 Calibration Summary.*
- 95-06: Biretta, Ritchie, and Rudloff, 08/95, *A Field Guide to WFPC2 Image Anomalies.*
- 95-05: Biretta, Ritchie, Baggett, MacKenty 04/96, *Wavelength / Aperture Calibration of the WFPC2 Linear Ramp Filters.*
- 95-04: Whitmore and Heyer, 07/95, *Demonstration Analysis Script for Performing Aperture Photometry.*
- 95-03: Whitmore and Wiggs, 07/95, *Charge Transfer Traps in the WFPC2*.
- 95-02: Gilmozzi, R. et al., 06/95, *The Geometric Distortion of the WFPC2 Cameras*.
- 95-01: Biretta and Sparks, 02/95, *WFPC2 Polarization Observations: Strategies, Apertures, and Calibration Plans.*
- 94-03: Burrows, C., 12/94, *WFPC2 Pipeline Calibration*.
- 94-01: Krist, J. and Burrows, C., 10/94, *Large Angle Scattering in WFPC2 and Horizontal "Smearing" Correction*.
- 93-01: Clampin, M., 3/93, *Polarizer Quad Nomenclature*.
- 92-06: Clampin, M., 12/92, *WFPC2 CCDs.*
- 92-05: Burrows, C., 11/92*WFPC2 AFM and POMM Actuation Algorithm.*
- 92-04: Trauger, J.T. et al., 7/92, *Science with the Second Wide Field and Planetary Camera*.

2. These documents may be requested by e-mail from `help@stsci.edu`.

- 92-03: Trauger, J.T. and Brown, D.I., 10/92, *WFPC2 Science Observation and Engineering Modes*.
- 92-02: Clampin, M., 9/92, *System Level Contamination Issues for WFPC2 and COSTAR*.

APPENDIX A:
Passband Plots

In This Appendix...

A.1 Passbands for each Filter in Isolation

F122M, F130LP, F160AW, F160BW, F165LP, F170W

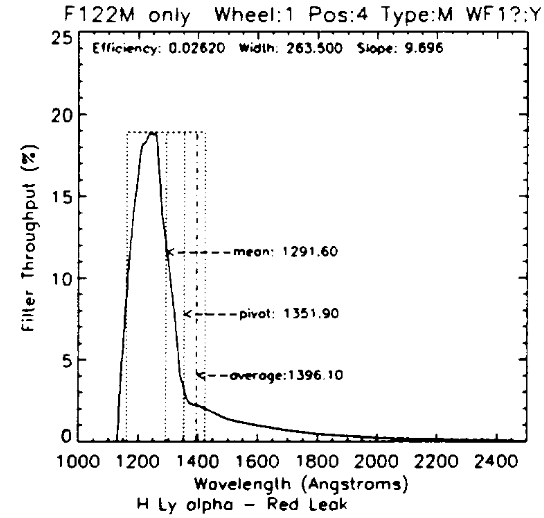

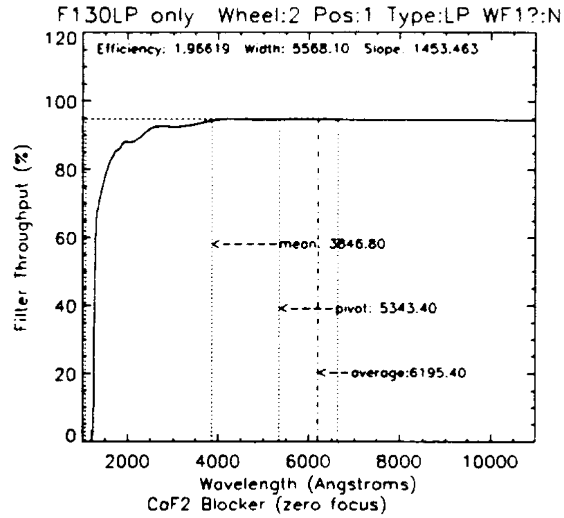

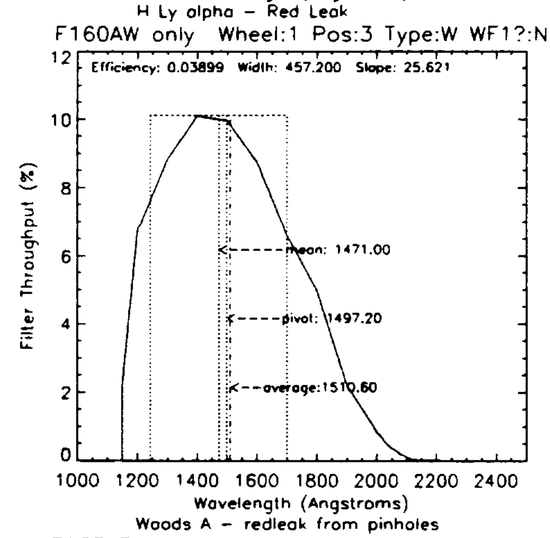

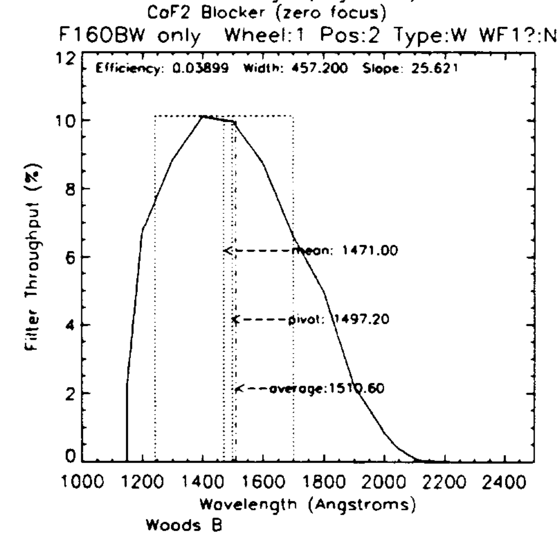

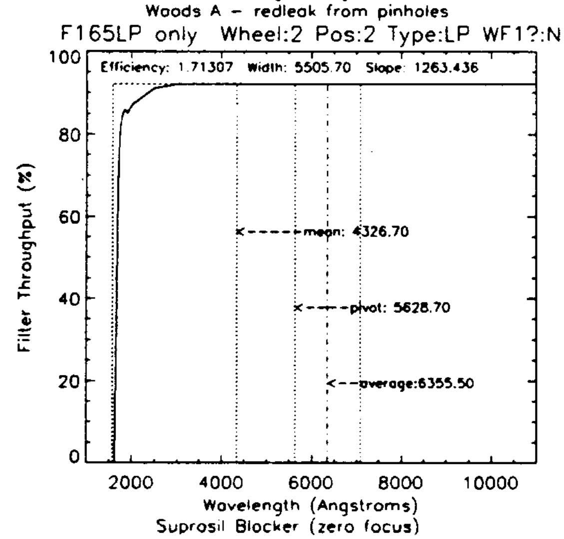

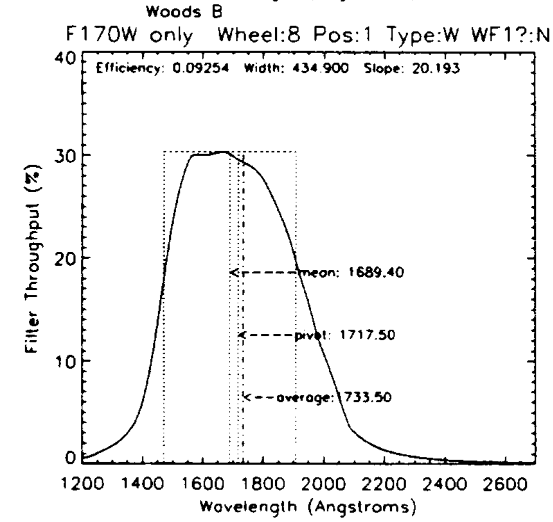

F185W, F218W, F255W, F300W, F336W, F343N

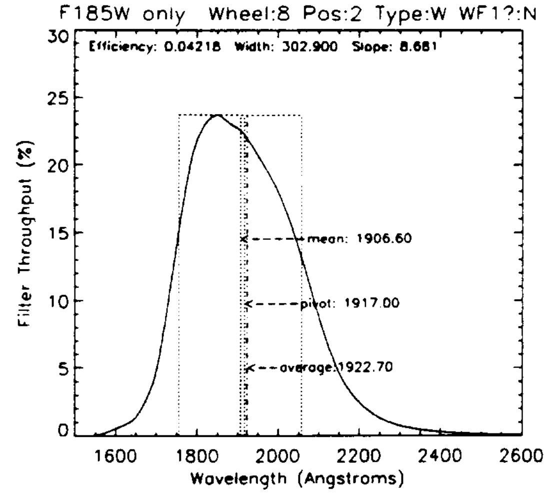

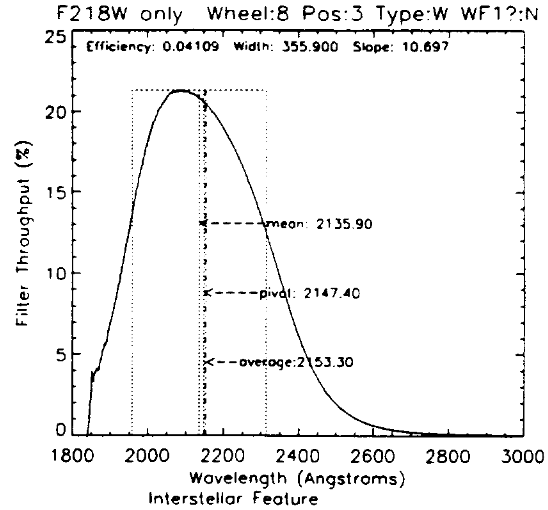

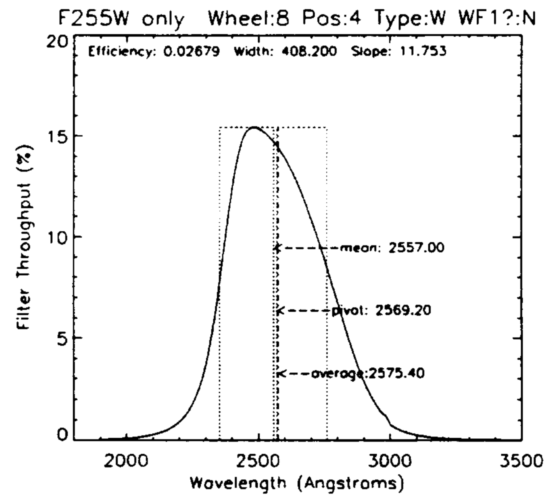

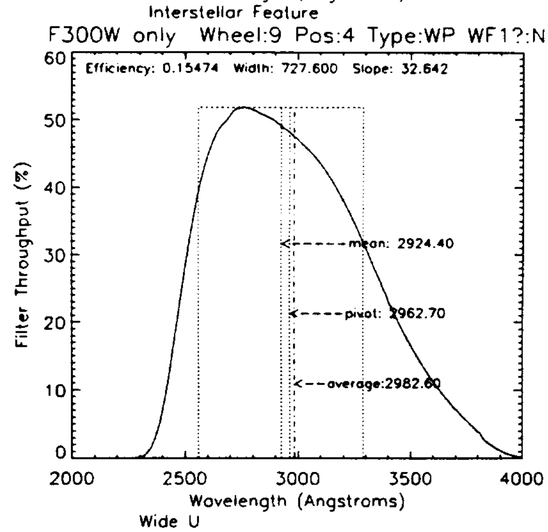

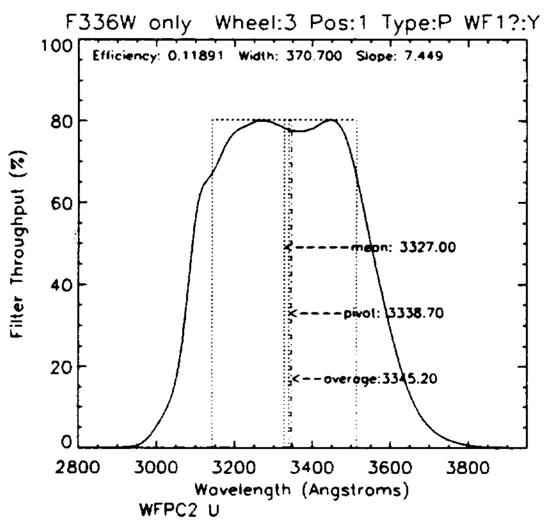

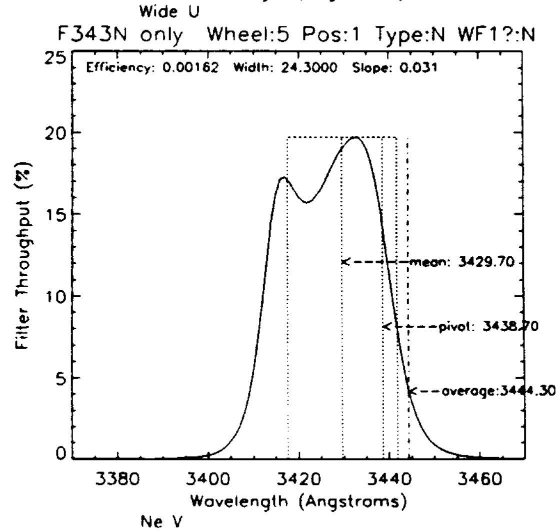

F375N, F380W, F390N, F410M, F437N, F439W

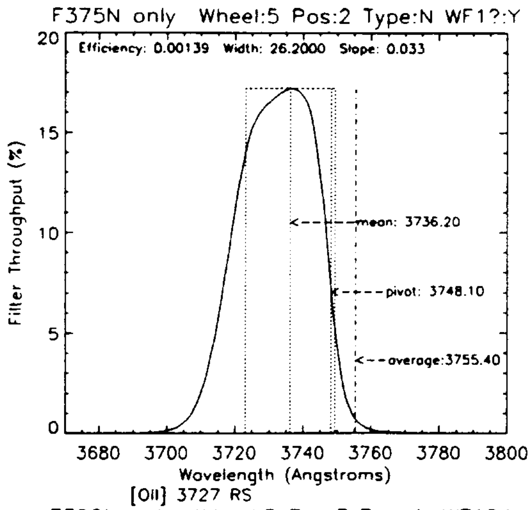

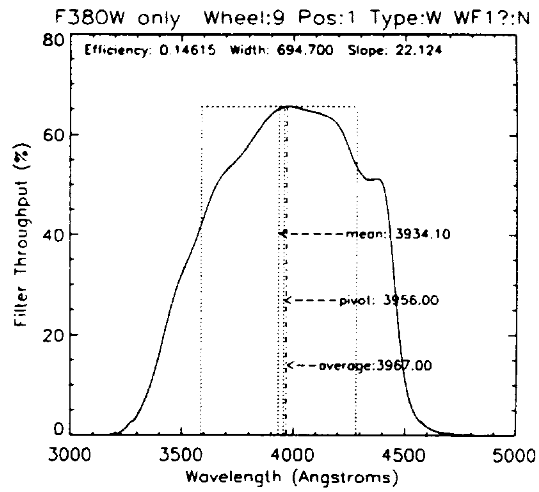

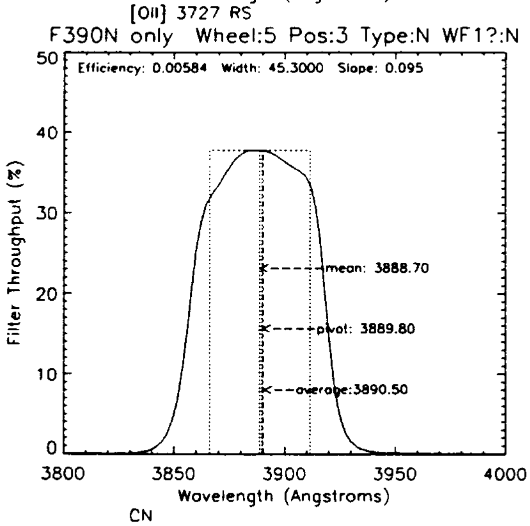

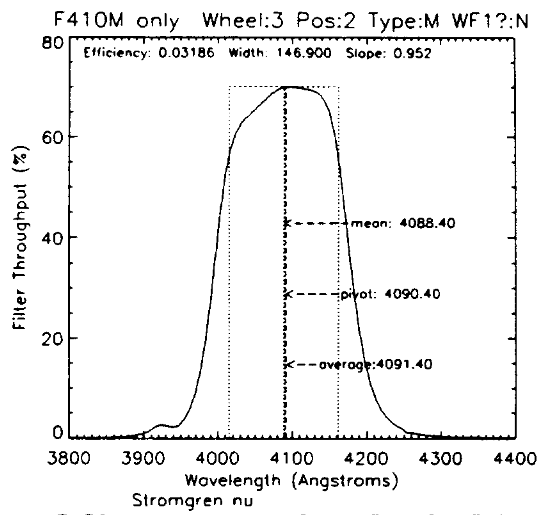

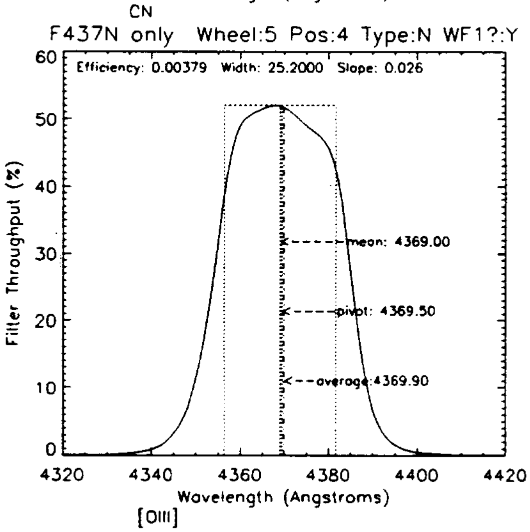

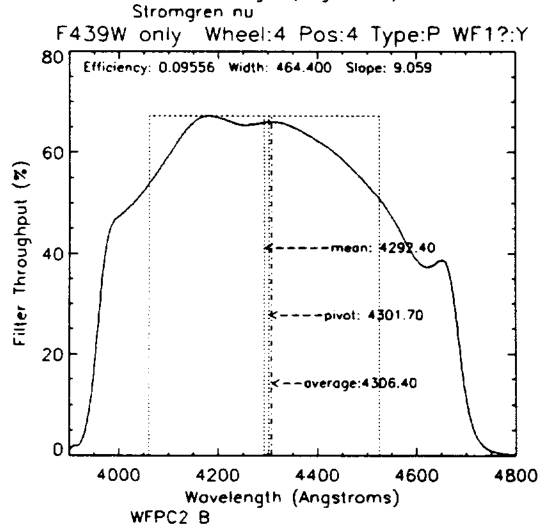

F450W, F467M, F469N, F487N, F502N, F547M

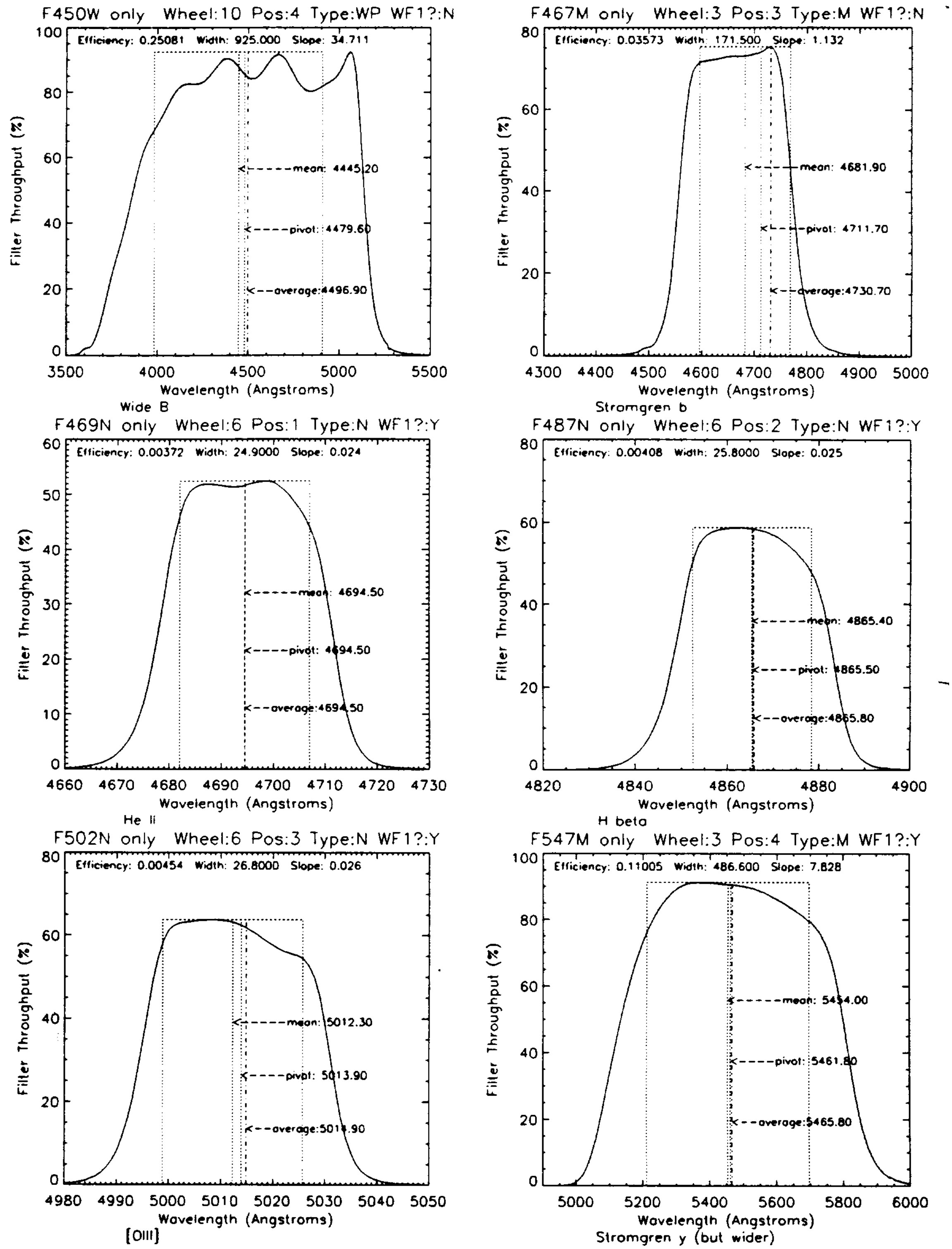

F555W, F569W, F588N, F606W, F622W, F631N

F555W only Wheel:9 Pos:2 Type:P WF1?:Y

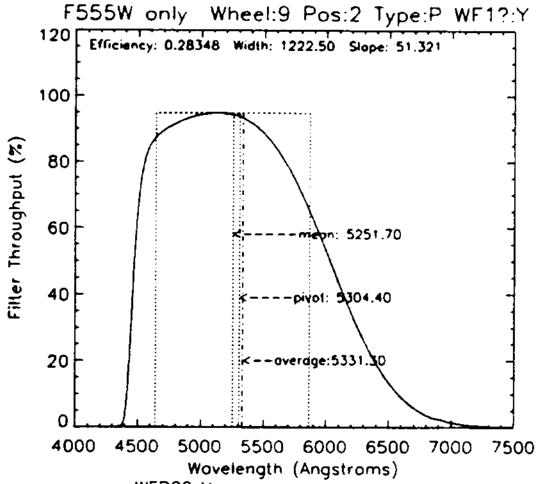

WFPC2 V

F569W only Wheel:4 Pos:2 Type:W WF1?:Y

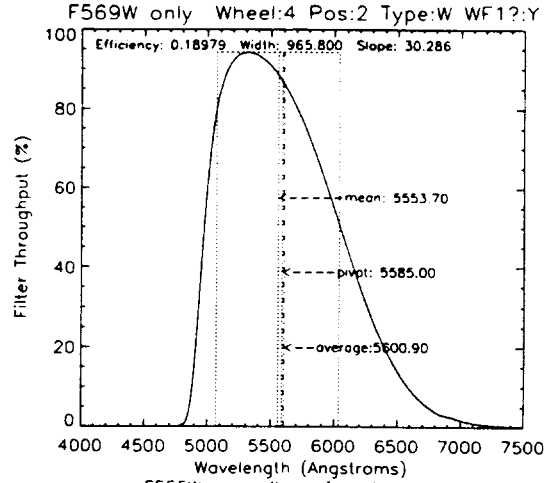

F555W generally preferred

F588N only Wheel:6 Pos:4 Type:N WF1?:Y

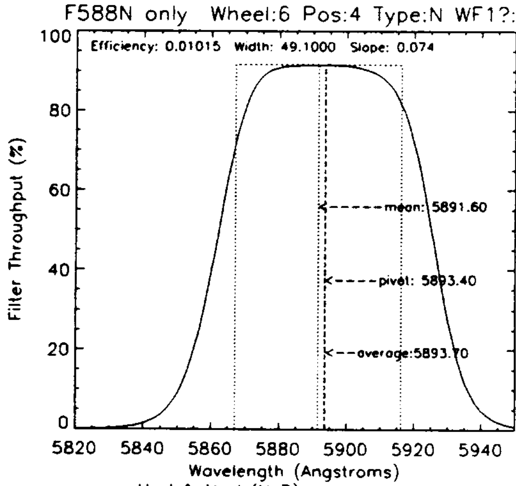

He I & Na I (NaD)

F606W only Wheel:10 Pos:2 Type:WP WF1?:Y

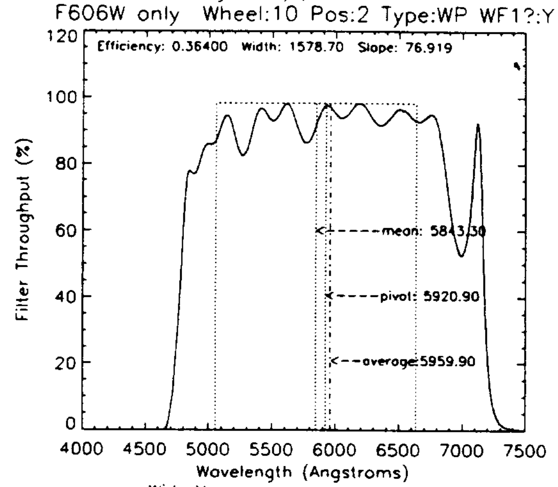

Wide V

F622W only Wheel:9 Pos:3 Type:W WF1?:Y

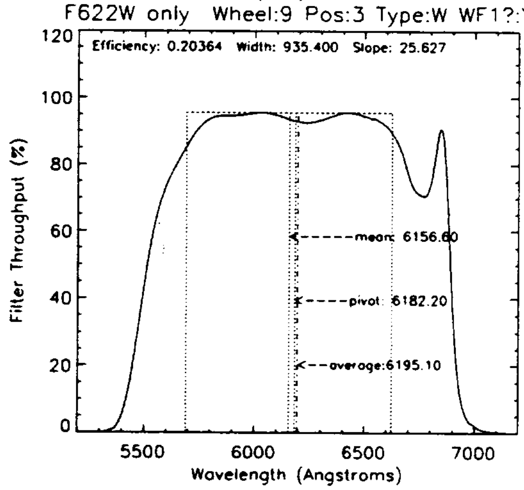

F631N only Wheel:7 Pos:1 Type:N WF1?:Y

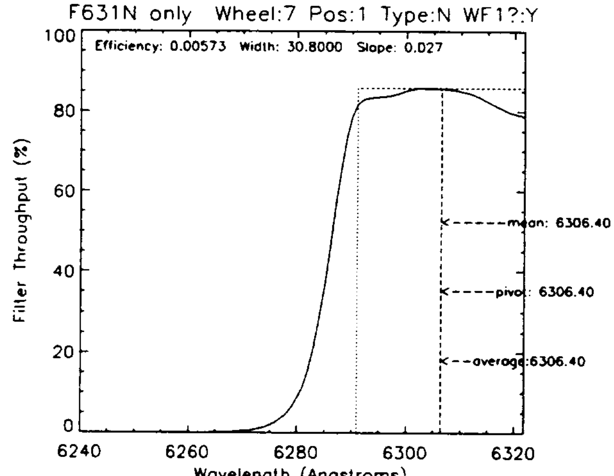

[OI]

F656N, F658N, F673N, F675W, F702W, F785LP

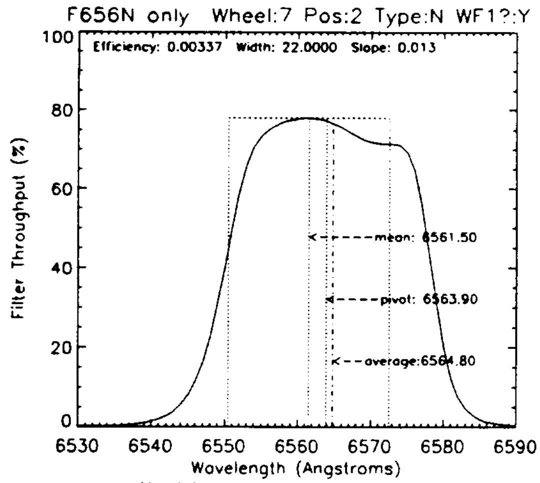

H−alpha

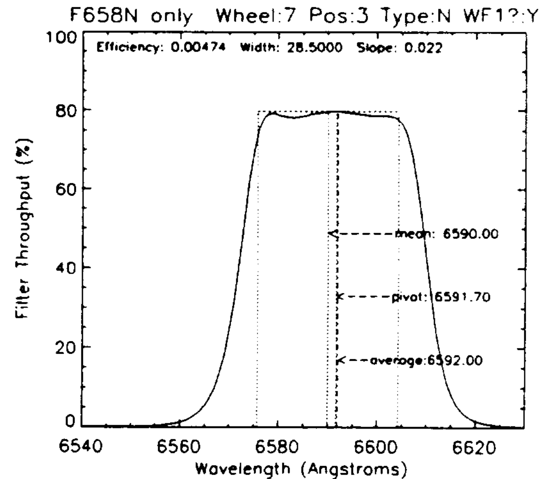

[NII]

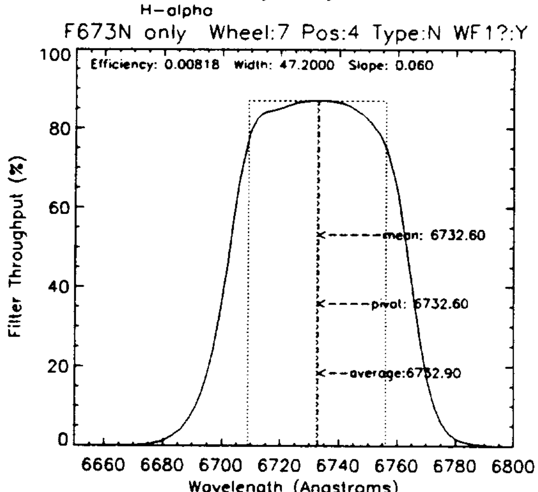

[SII]

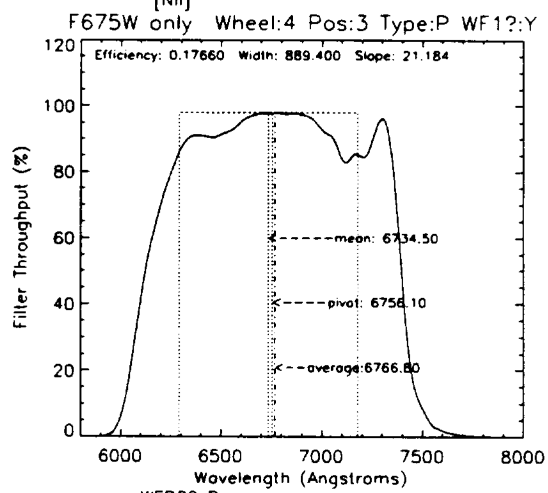

WFPC2 R

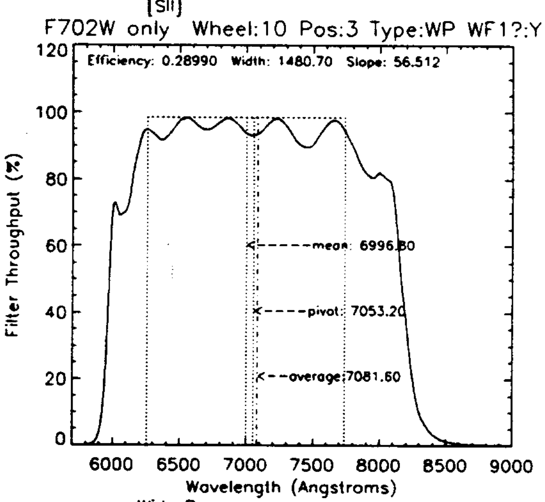

Wide R

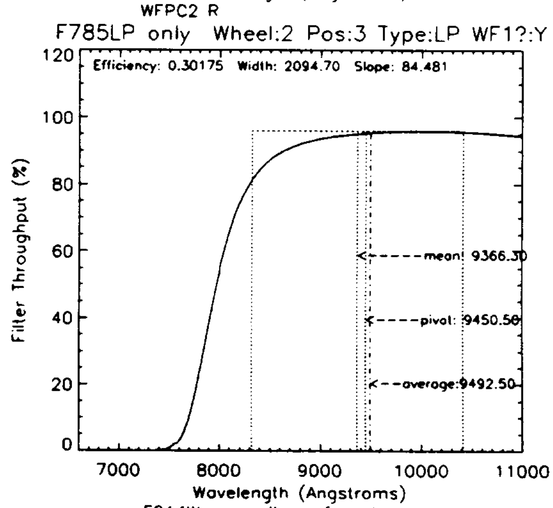

F814W generally preferred

F791W, F814W, F850LP, F953N, F1042M, FQUVN-A

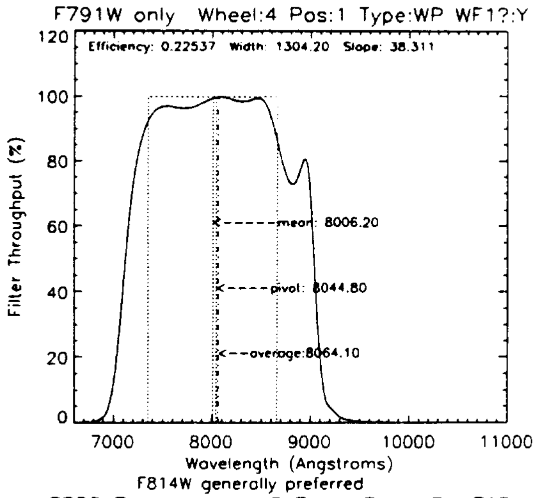

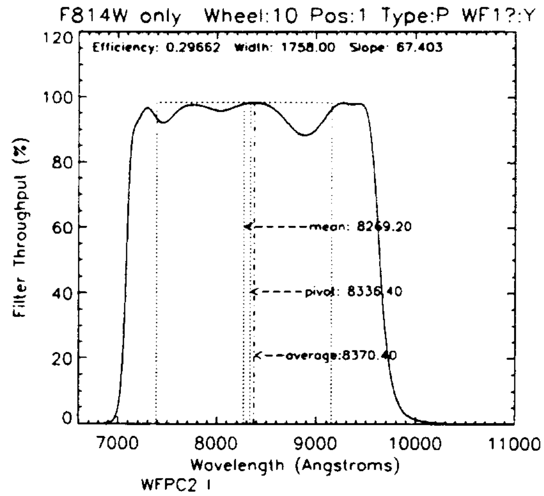

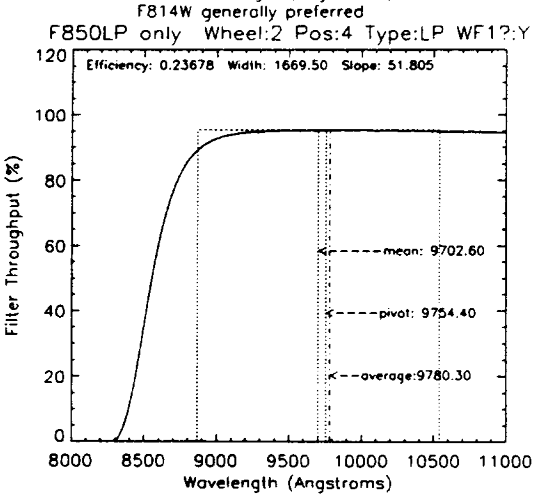

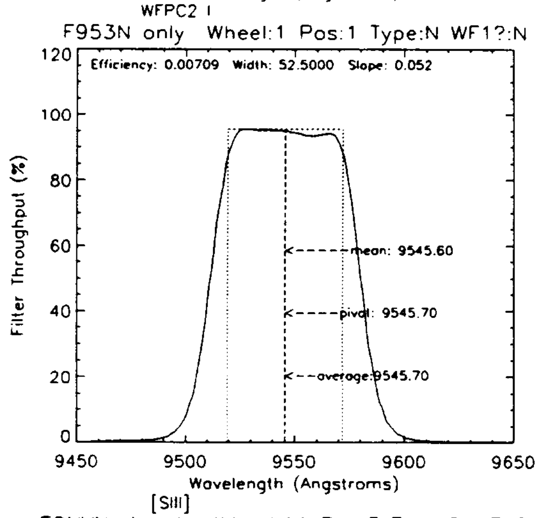

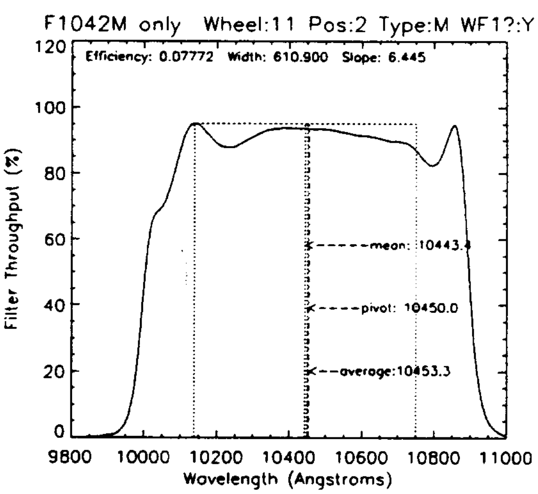

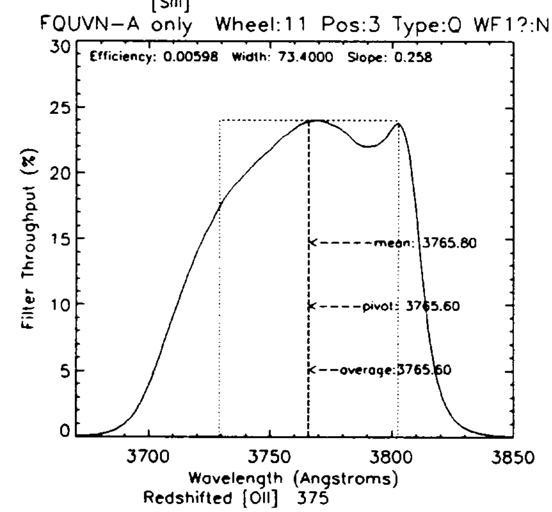

FQUVN-B, C and D, FQCH4N-A, B and C

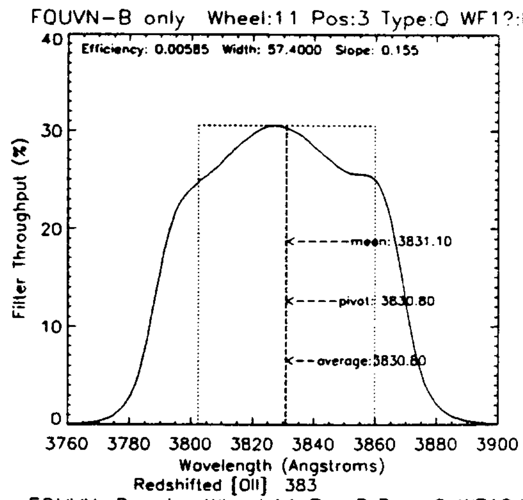

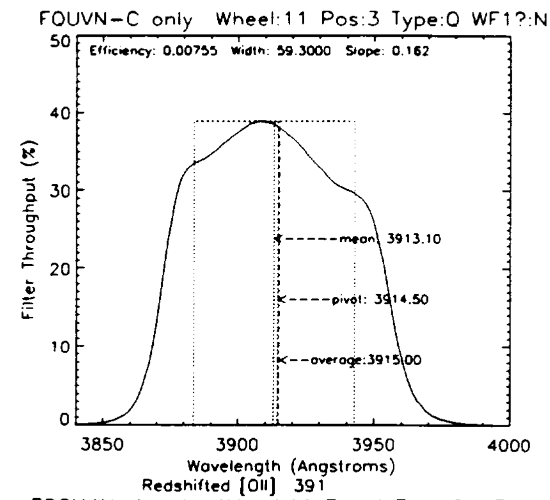

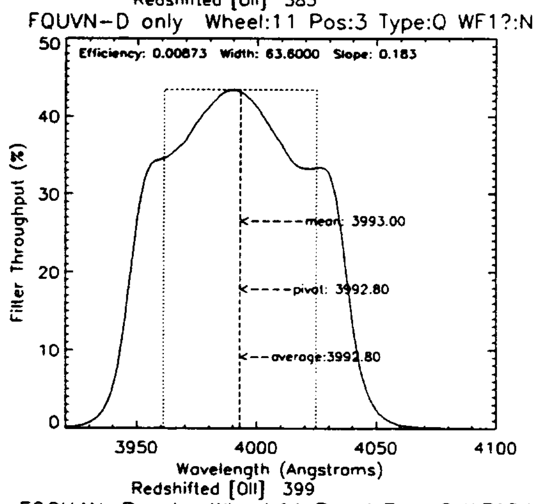

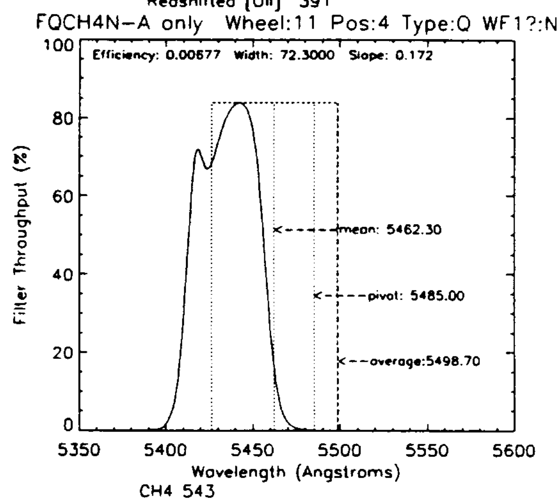

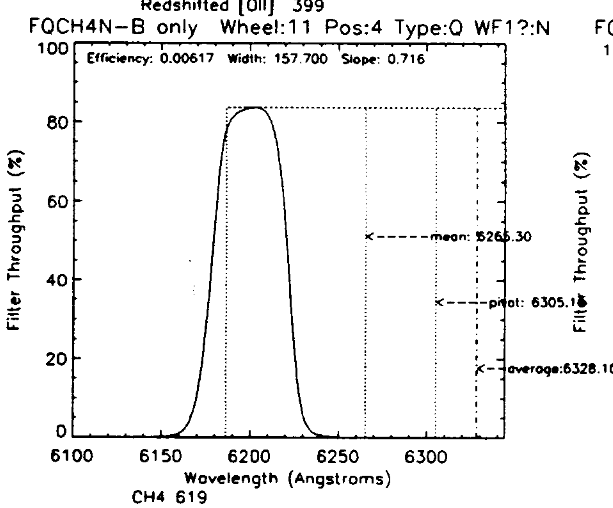

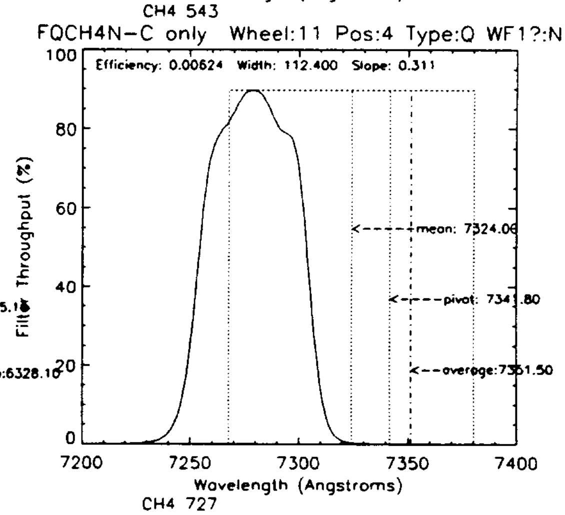

FQCH4N-D, Parallel and Perpendicular Polarizers

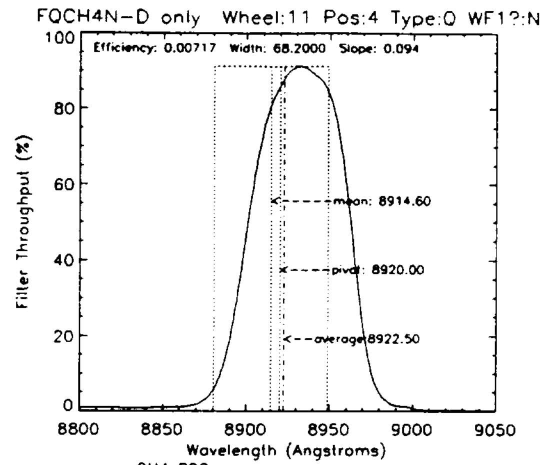

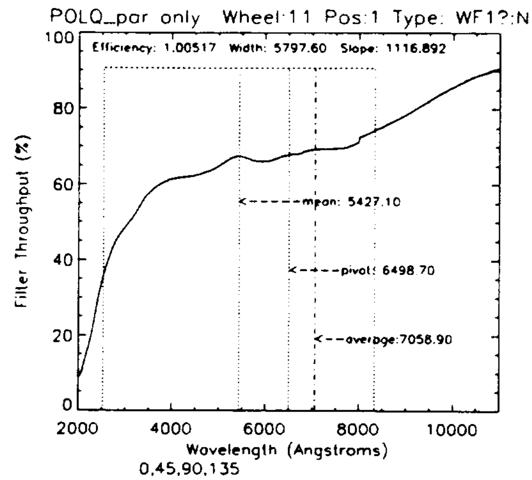

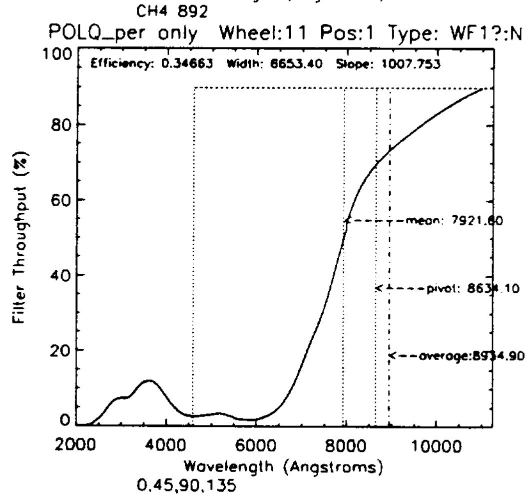

A.2 Passbands including the System Response

F122M, F130LP, F160AW, F160BW, F165LP, F170W

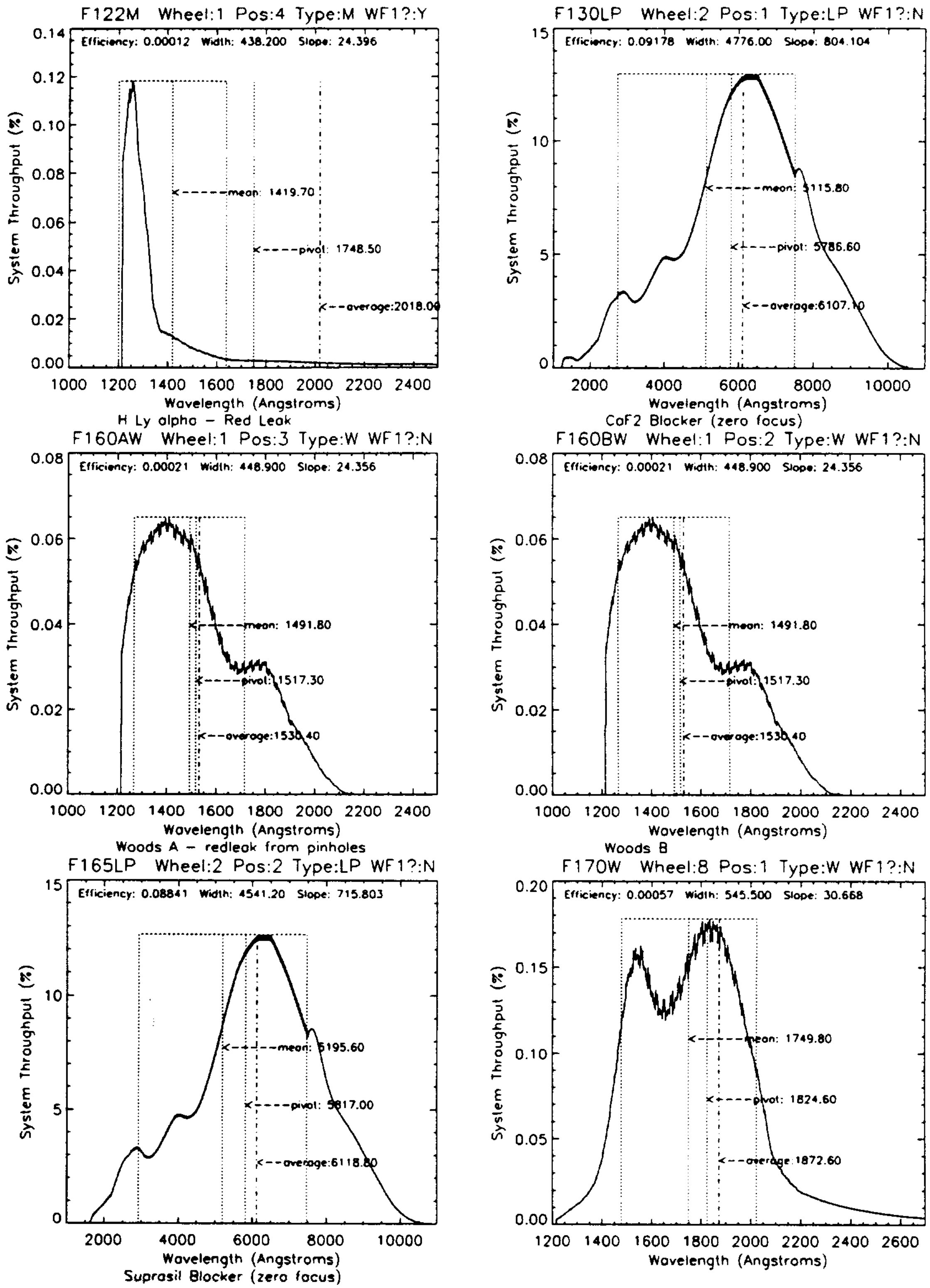

F185W, F218W, F255W, F300W, F336W, F343N

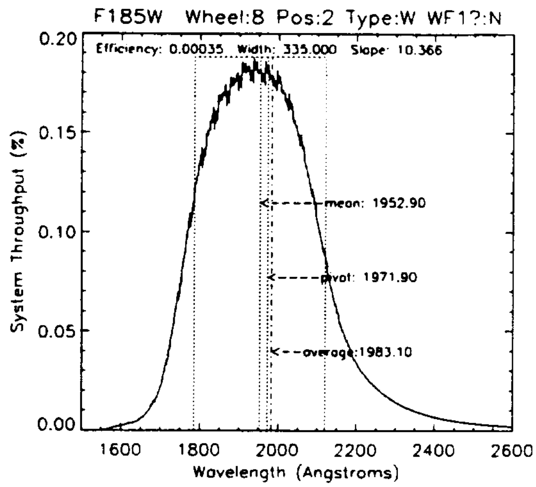

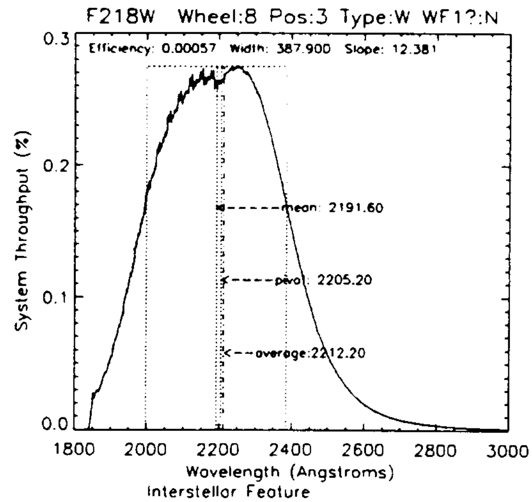

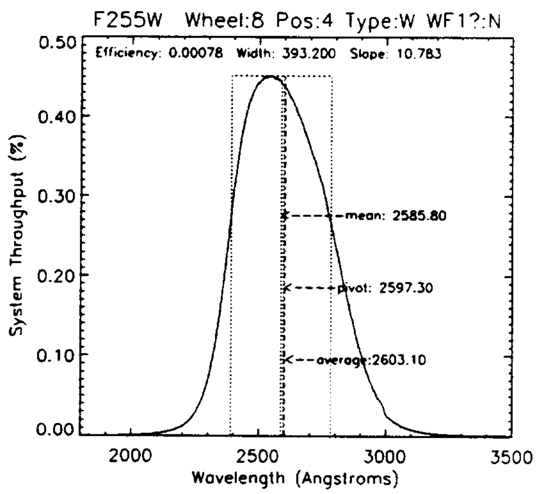

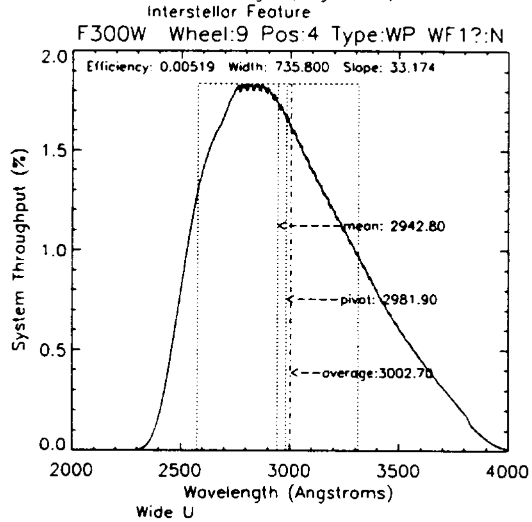

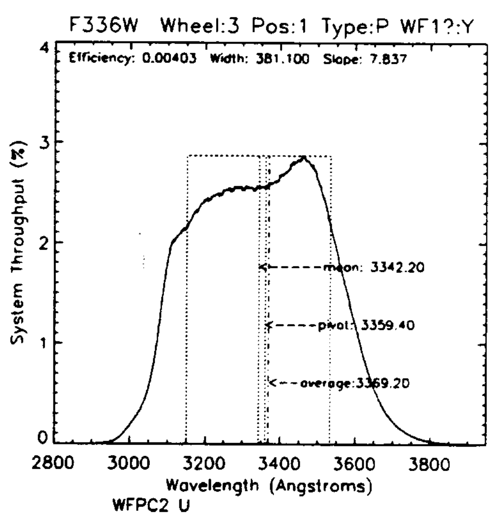

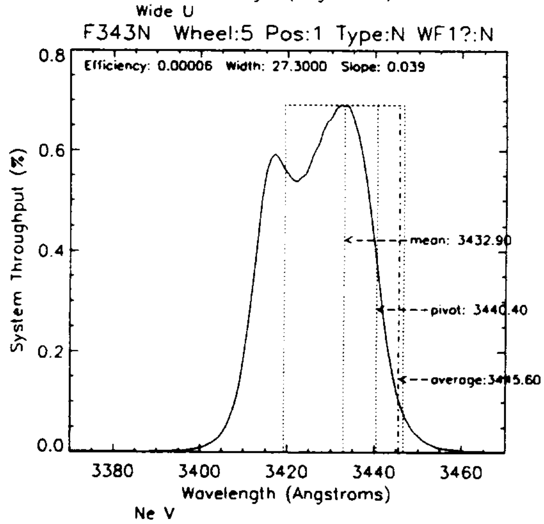

F375N, F380W, F390N, F410M, F437N, F439W

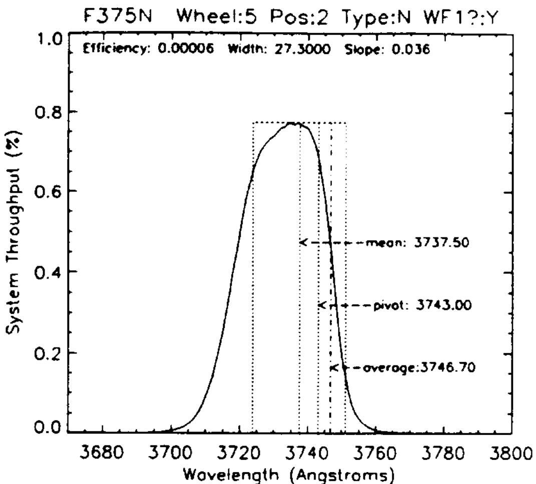

[OII] 3727 RS

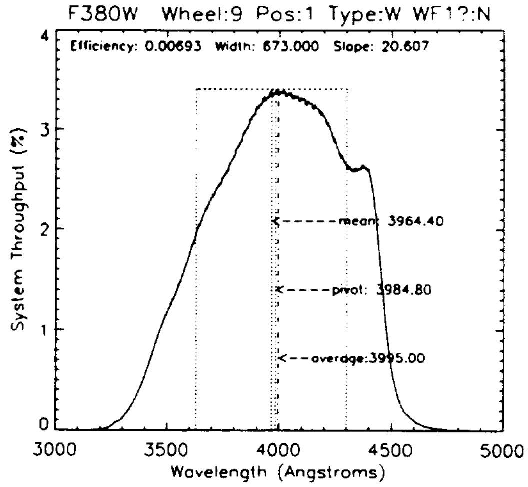

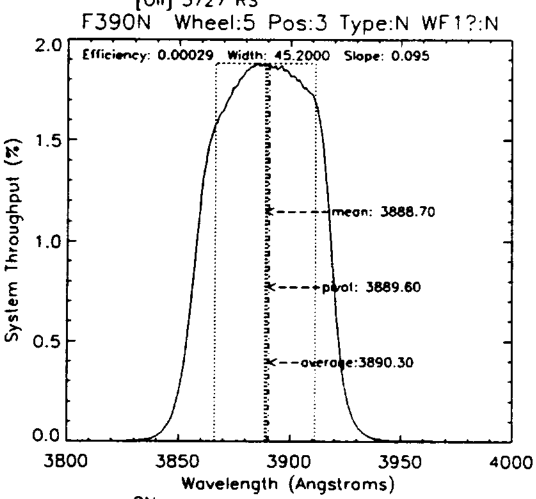

CN

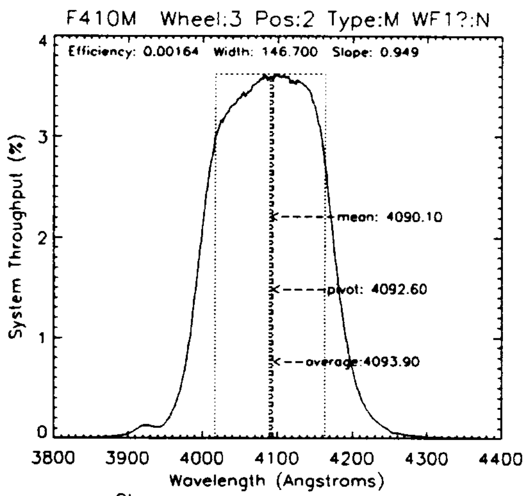

Stromgren nu

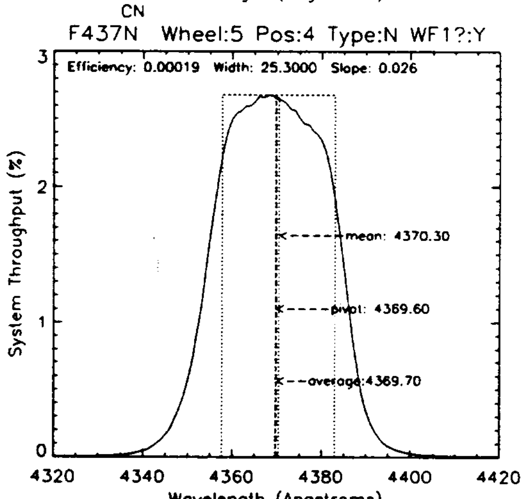

[OIII]

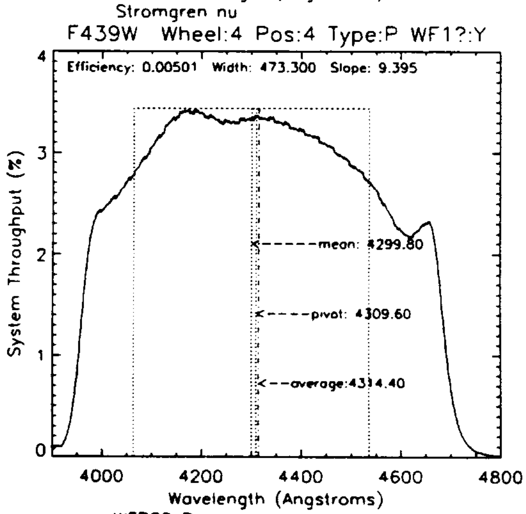

WFPC2 B

F450W, F467M, F469N, F487N, F502N, F547M

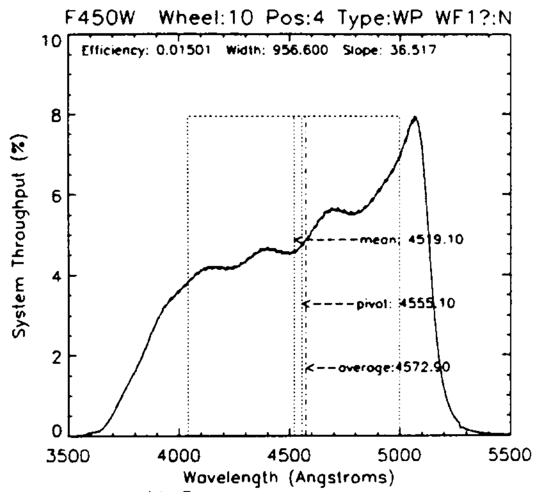

Wide B

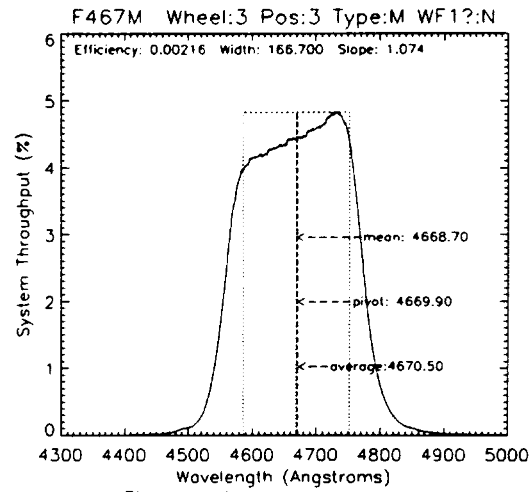

Stromgren b

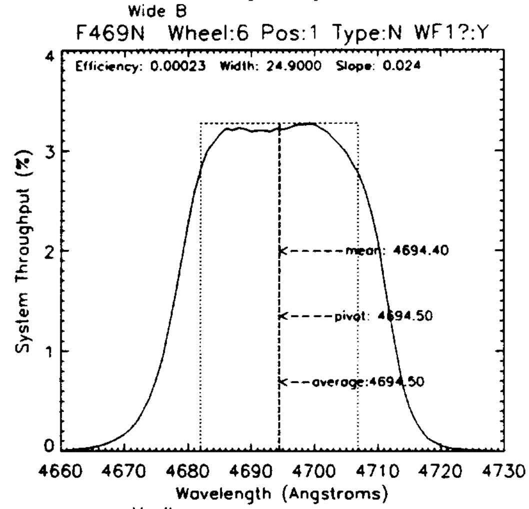

He II

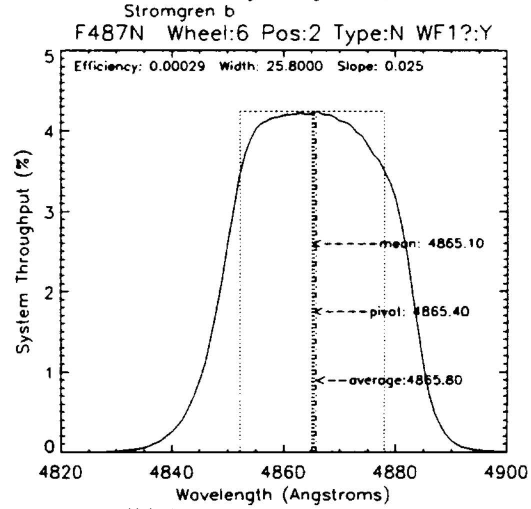

H beta

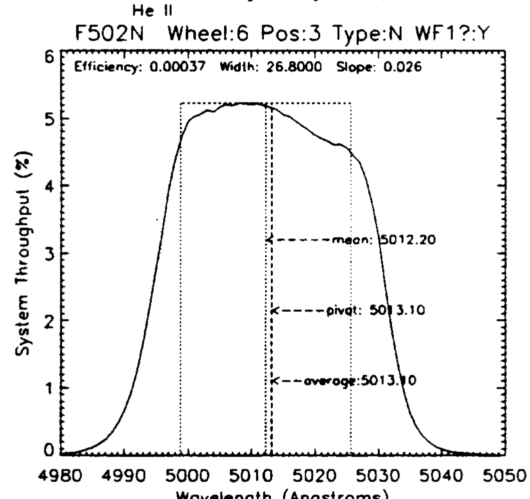

[OIII]

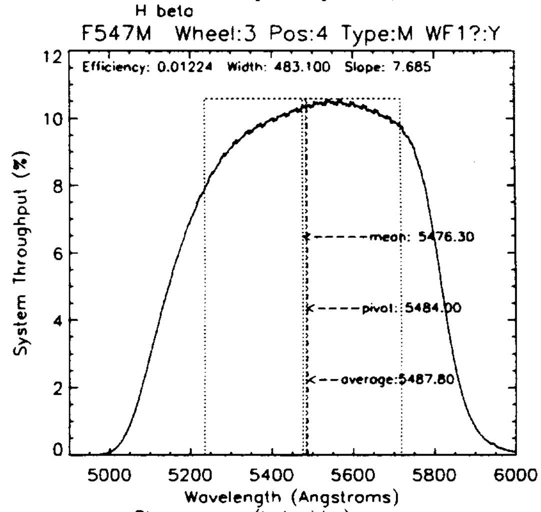

Stromgren y (but wider)

F555W, F569W, F588N, F606W, F622W, F631N

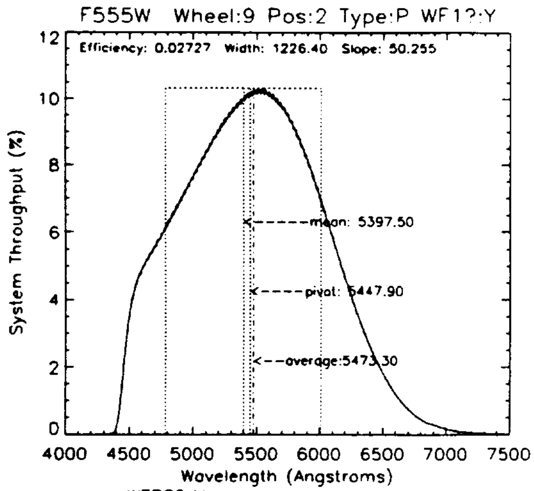

WFPC2 V

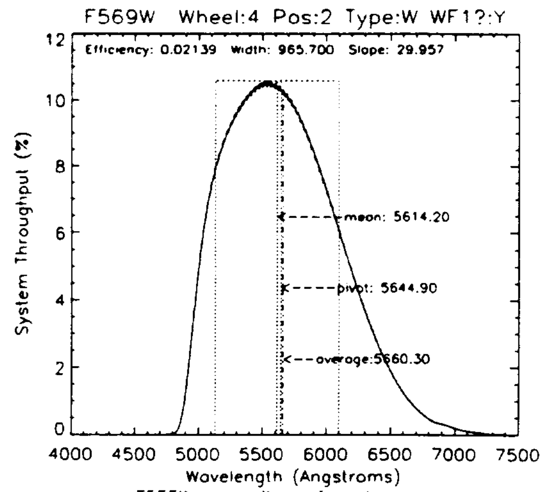

F555W generally preferred

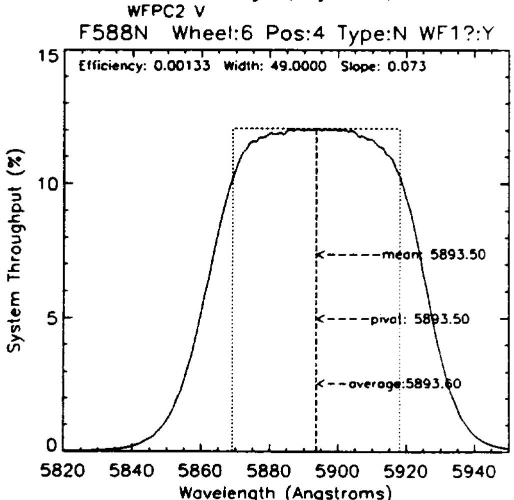

He I & Na I (NaD)

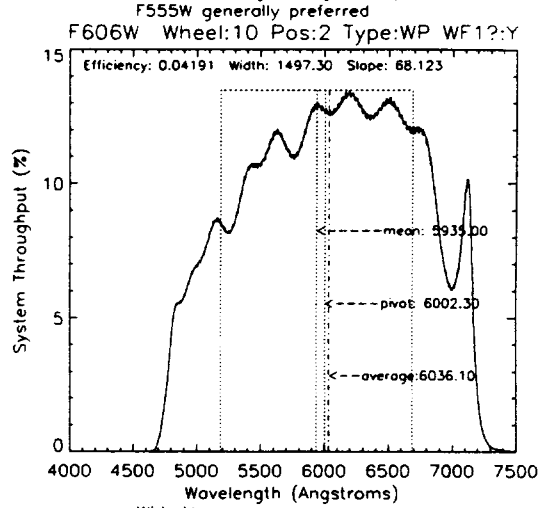

Wide V

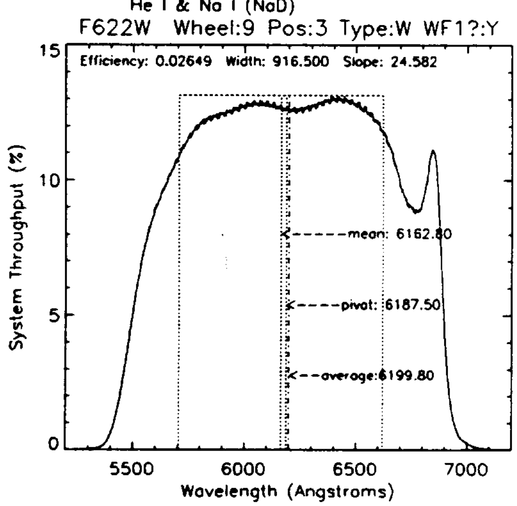

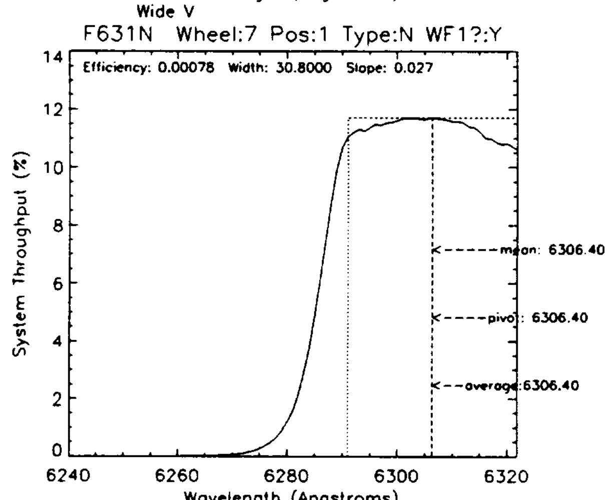

[OI]

F656N, F658N, F673N, F675W, F702W, F785LP

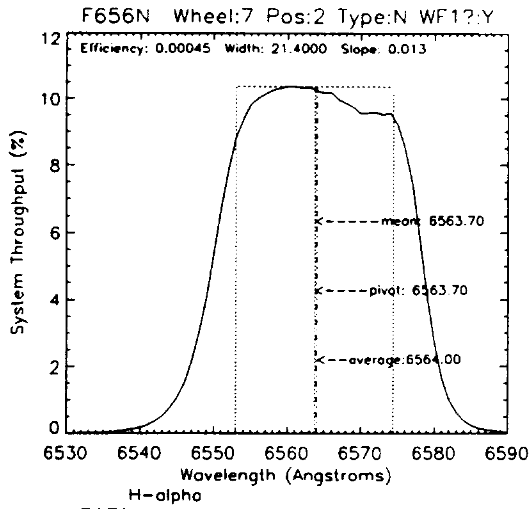

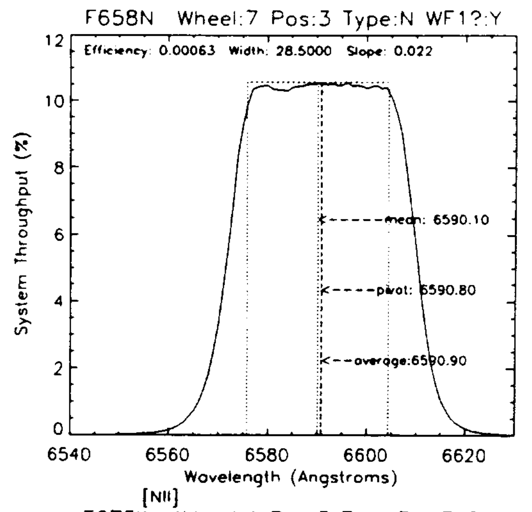

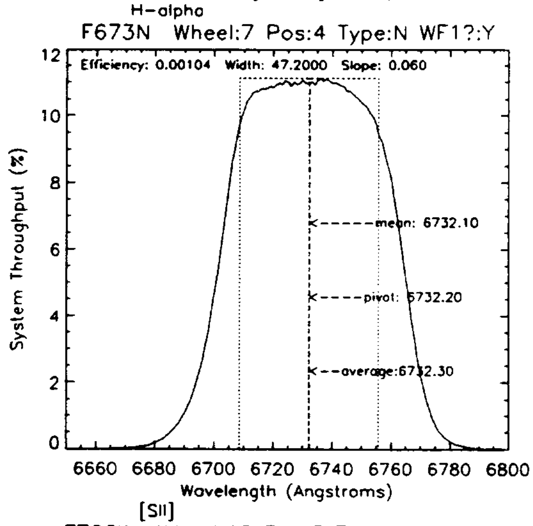

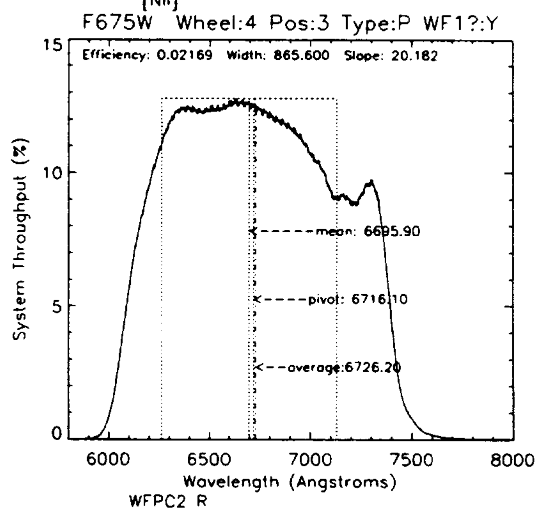

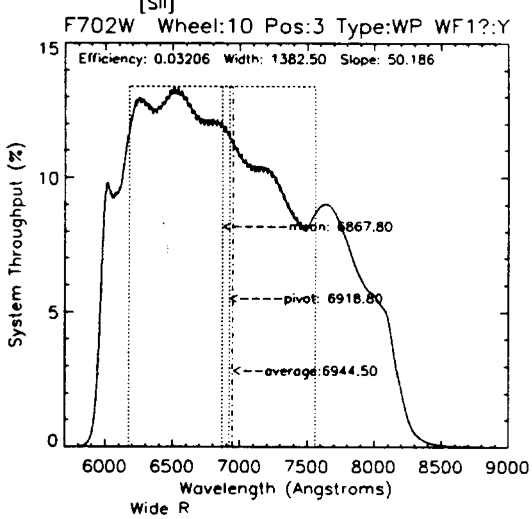

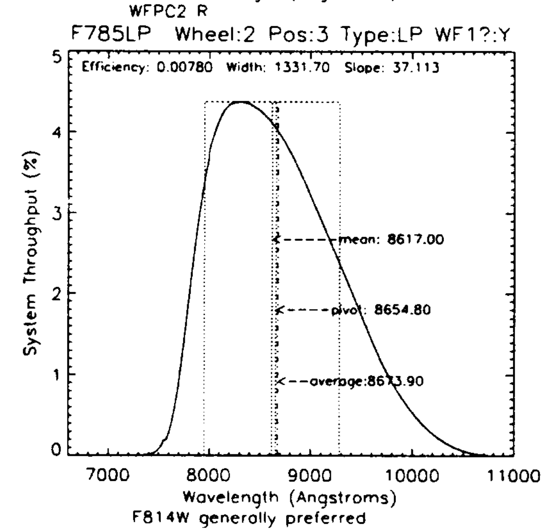

F791W, F814W, F850LP, F953N, F1042M, FQUVN-A

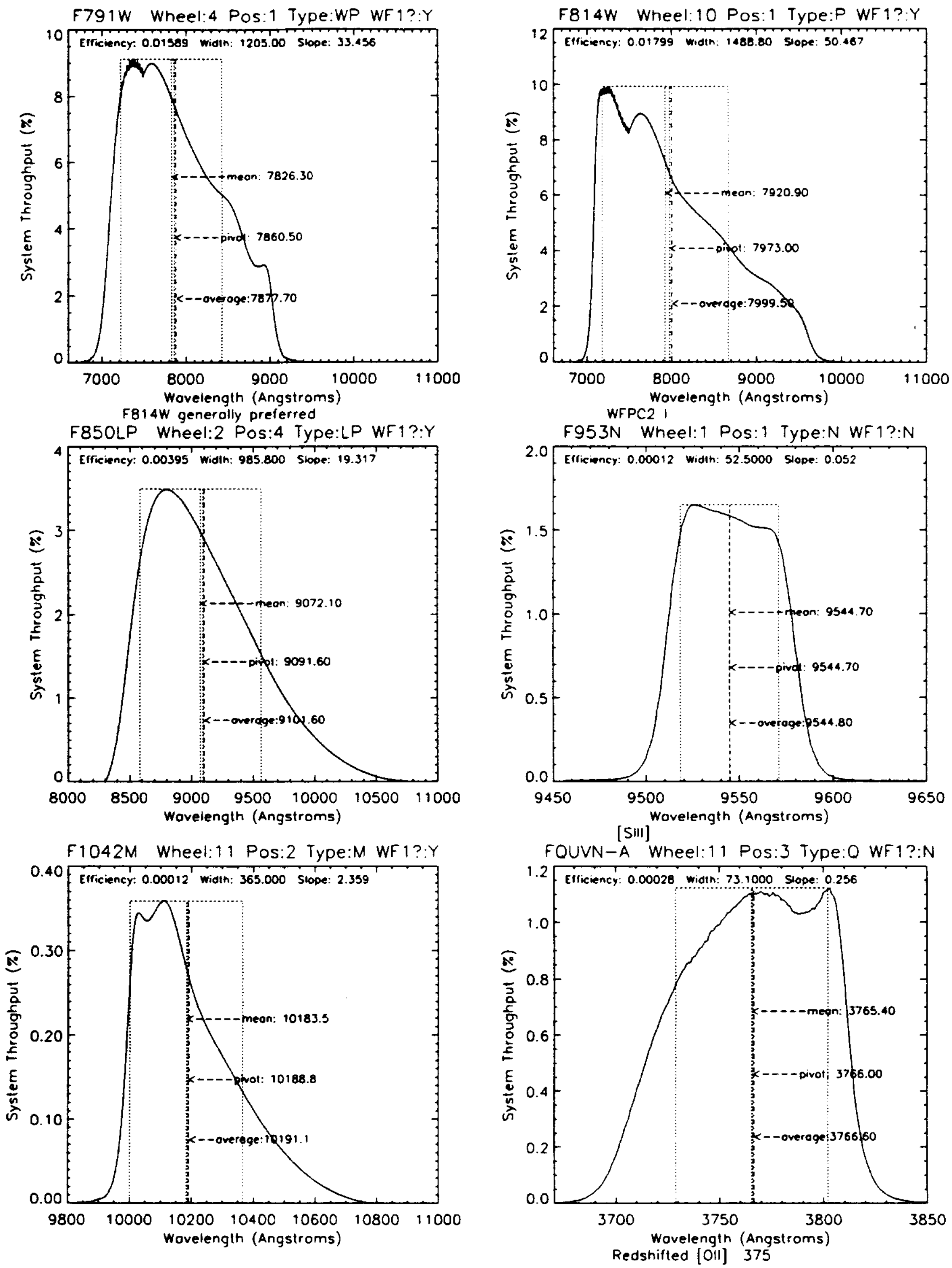

FQUVN-B, C and D, FQCH4N-A, B and C

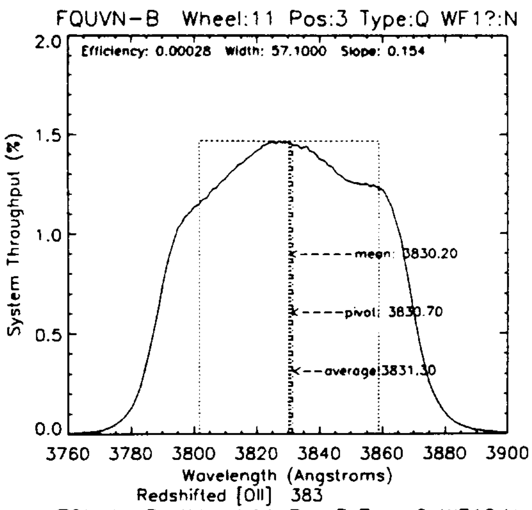

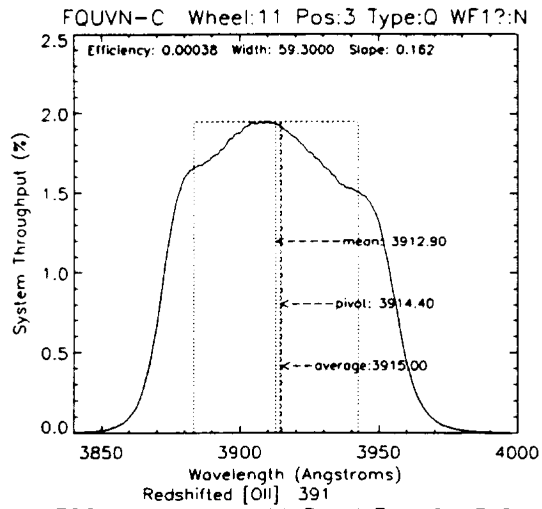

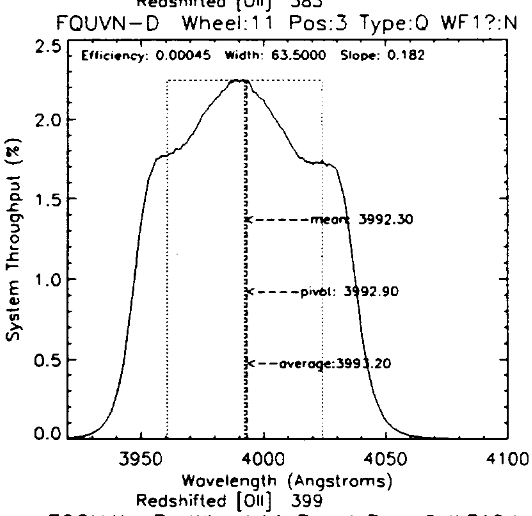

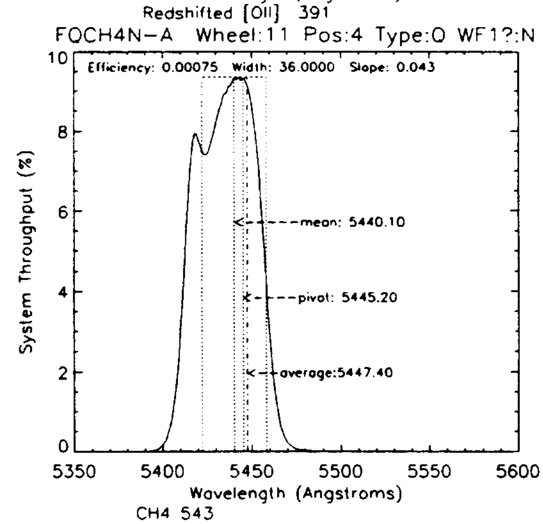

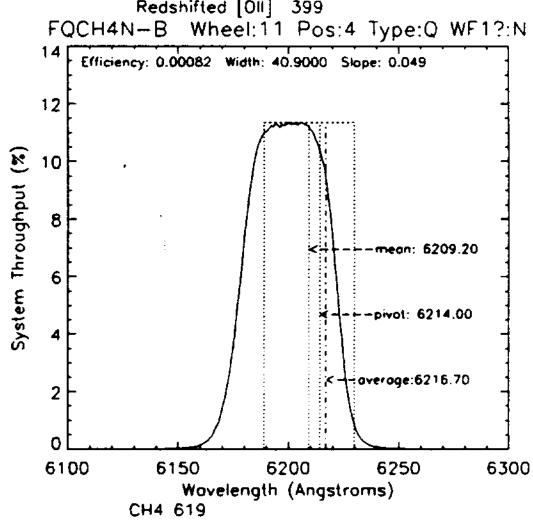

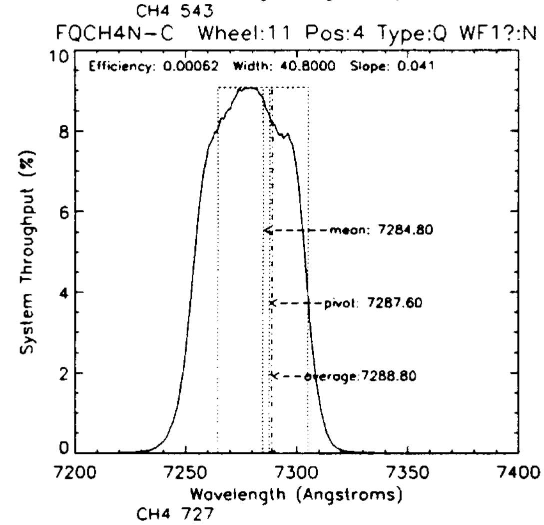

FQCH4N-D, Parallel and Perpendicular Polarizers

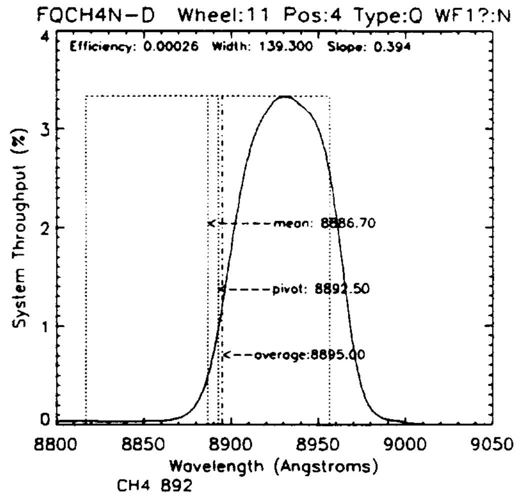

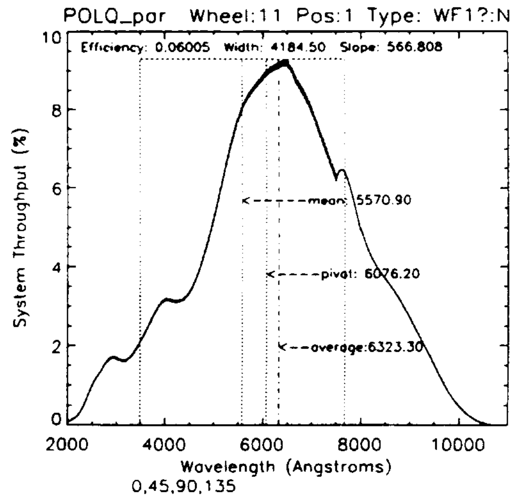

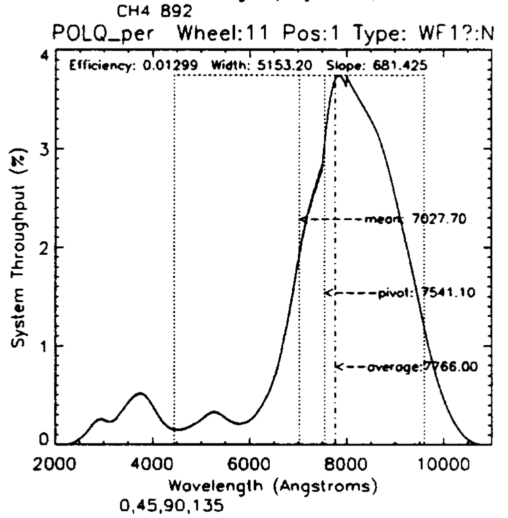

A.3 Normalized Passbands including the System Response

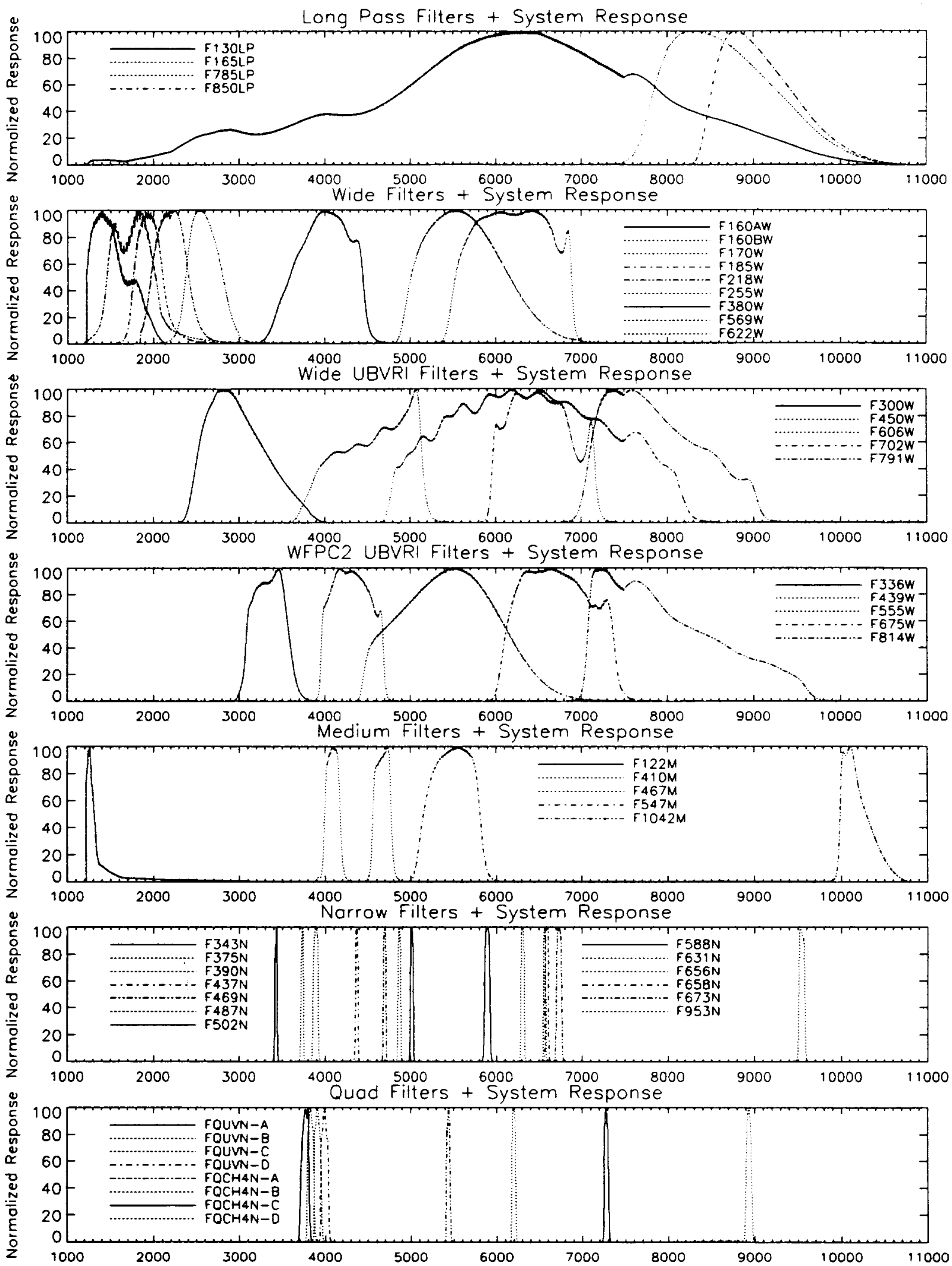

APPENDIX B:
Point Source SNR Plots

In This Appendix...

B.1 Plots for Estimating Point Source SNR

In this section we present plots which may be used to rapidly estimate signal-to-noise ratio (SNR) for point sources with stellar spectra observed through popular WFPC2 filters. Plots are given for filters F160BW, F218W, F255W, F300W, F336W, F410M, F439W, F502N, F547M, F555W, F606W, F675W, F702W, and F814W. These plots assume that the data will be analyzed by PSF fitting, which optimizes the SNR in the background noise limited case. They also assume an average sky background of V=22.9 mag arcsec^{-2}. These plots do not explicitly include SNR reduction due to CR-SPLITing when the read noise dominates, but this effect is easily included as described below.

In situations requiring more detailed calculations (non-stellar spectra, extended sources, other sky background levels, don't know target V magnitude, etc.), the WFPC2 Exposure Time Calculator tool, located on the WFPC2 WWW pages, should be used instead.

One uses these plots as follows:

1. Examine Table B.1 and find the spectral type and wavelength of the desired filter (e.g. F555W ≈5500Å). Interpolate in the Table to get AB_ν.
2. Sum the V magnitude of the target and AB_ν derived from the Table.
3. Find the appropriate plot for the filter in question, and locate $V+AB_\nu$ on the horizontal axis. Then read off the SNR for the desired exposure time, or vice-versa.
4. To get accurate values for CR-SPLIT exposures, one should use the sub-exposure time when consulting the plot, and then multiply the resulting SNR by $\sqrt{N}$, where N is the number of sub-exposures to be averaged.

There are separate lines for PC1 (light lines) and the WFC (heavy lines), as well as for ATD-GAIN=7 (default, solid lines), and ATD-GAIN=15 (dashed lines).

Dotted lines across the top of each plot indicate the onset of saturation. There are lines for saturation of the ATD-GAIN=7 setting (G=7), saturation of the ATD-GAIN=15 setting (G=15), and finally a line where blooming starts (top-most line for given camera).

We now give a sample SNR calculation using these plots. Consider a V=20 star of spectral class G0, for which we want to derive the SNR for 1200s CR-SPLIT exposure in F555W on PC1. We look up the G0 spectral class and F555W filter (5500Å) in Table B.1, and obtain AB_ν=0.02. We thus have V+AB_ν=20.02. We look at Figure B.10 and find this value on the horizontal axis. We locate exposure time 600s (one-half of the total 1200s CR-SPLIT exposure), and find SNR~200. For the total 1200s exposure the SNR would be $200\sqrt{2} = 280$. This exposure is well below the saturation lines in the plot, so saturation is not a concern. If instead, the star had V=19, we would be approaching the "Saturate G=7 PC" line indicating A-to-D converter saturation at gain 7, and so would want to specify ATD-GAIN=15.

Table B.1: AB_ν as a Function of Wavelength. AB_ν is defined as a color-dependent correction from V magnitude to AB magnitude at frequency ν. Wavelength (Å) runs along the top; spectral classes run down the leftmost column. The second column contains B-V. See Section 6.3.

	B-V	1500	2000	2500	3000	3500	4000	4500	5000	6000	7000	8000	9000	10000
sky	1.10	2.45	5.46	5.46	3.12	2.00	1.03	0.55	0.18	-0.11	-0.33	-0.55	-0.65	-0.75
B0	-0.31	-1.60	-1.50	-1.20	-0.78	-0.62	-0.46	-0.36	-0.22	0.16	0.46	0.76	0.96	1.17
A0	0.00	2.22	1.35	1.11	1.21	1.00	-0.23	-0.16	-0.09	0.11	0.22	0.33	0.36	0.4
F0	0.27	7.22	4.10	3.11	1.99	1.38	0.29	0.06	0.03	0.03	0.05	0.08	0.09	0.1
G0	0.58	8.9	6.35	4.61	2.46	1.63	0.67	0.26	0.08	-0.04	-0.12	-0.21	-0.23	-0.25
K0III	1.07	13	10.3	8.11	5.46	2.13	1.16	0.46	0.2	-0.24	-0.42	-0.61	-0.66	-0.72
M0III	1.60	15	12.3	9.36	6.21	4.63	2.26	0.96	0.51	-0.46	-0.76	-1.06	-1.12	-1.19
gE	1.00	6.82	6.41	5.43	3.63	2.49	1.40	0.55	0.21	-0.19	-0.52	-0.81	-1.07	-1.29
Sa	0.80	5.40	4.80	4.10	3.00	2.01	1.12	0.44	0.19	-0.17	-0.44	-0.7	-0.95	-1.16
Sbc	0.60	4.03	3.18	2.86	2.46	1.54	0.84	0.34	0.17	-0.14	-0.37	-0.6	-0.84	-1.04
Scd	0.45	2.67	2.29	2.15	1.76	1.35	0.65	0.28	0.13	-0.11	-0.26	-0.39	-0.47	-0.58
Ir I	0.30	1.77	1.40	1.36	1.24	0.94	0.43	0.34	0.17	0.13	-0.04	-0.21	-0.33	-0.45

Figure B.1: Point Source SNR vs. V+AB$_\nu$ for F160BW Filter.

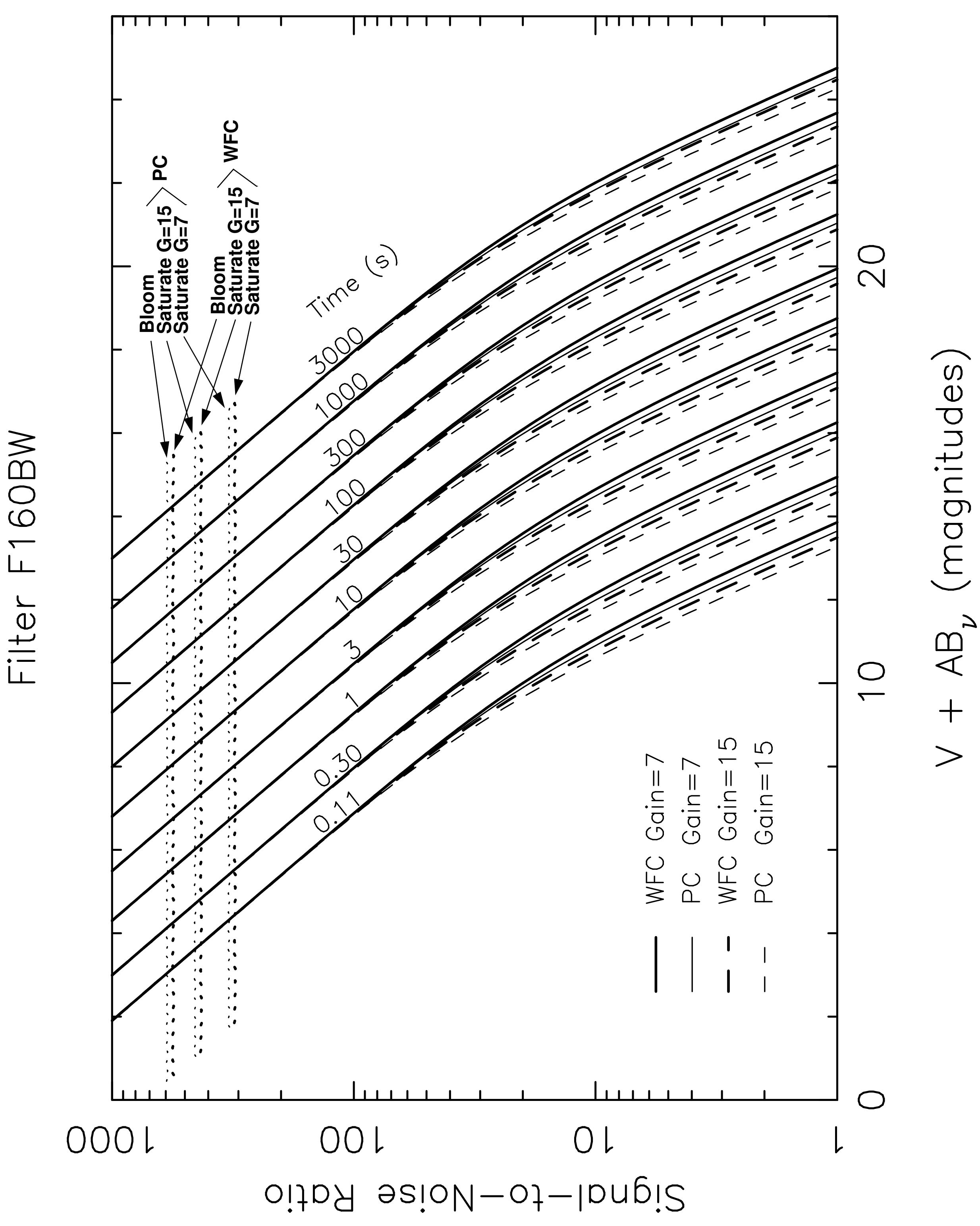

Figure B.2: Point Source SNR vs. V+AB$_\nu$ for F218W Filter.

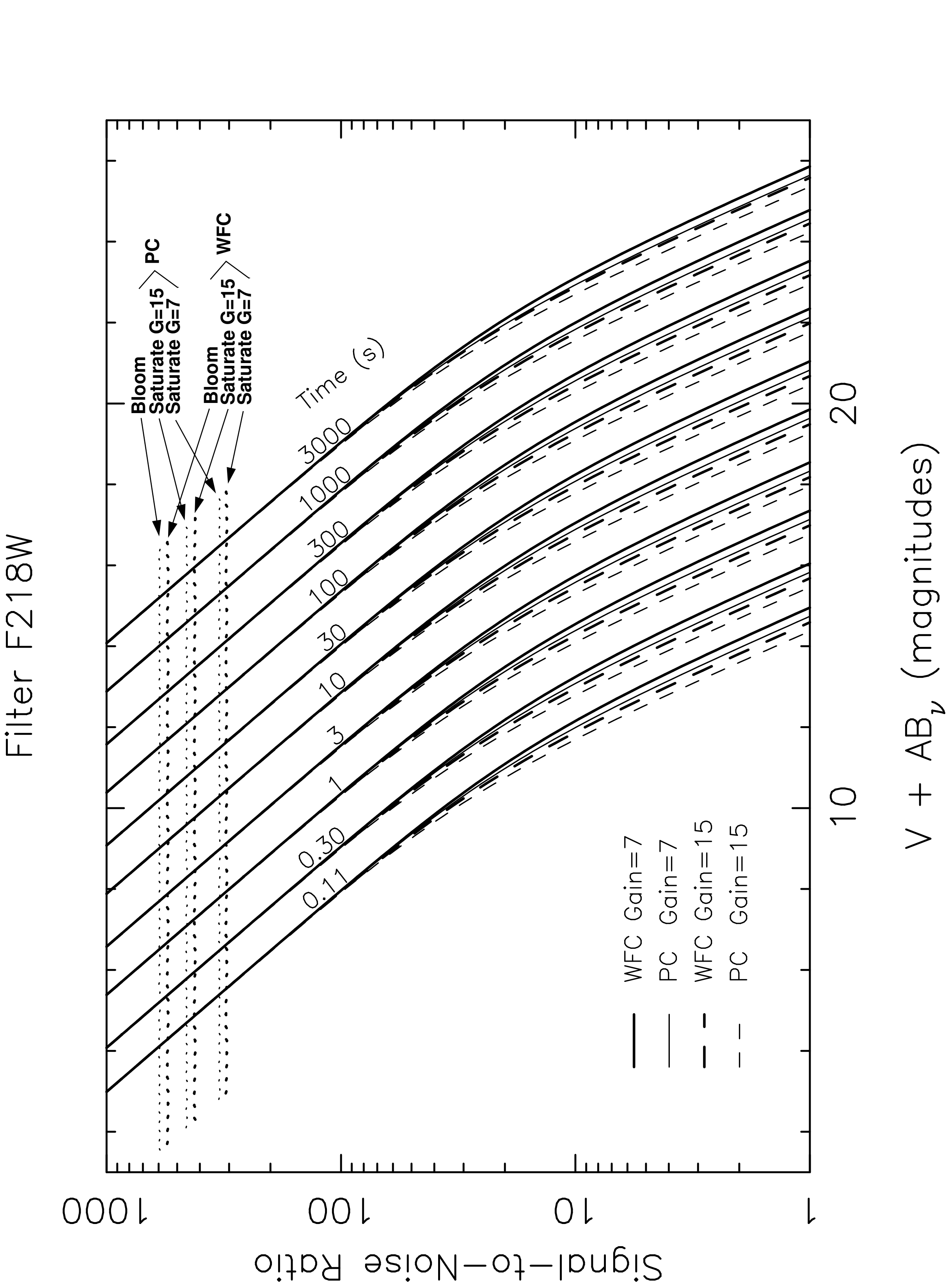

Figure B.3: Point Source SNR vs. V+AB$_\nu$ for F255W Filter.

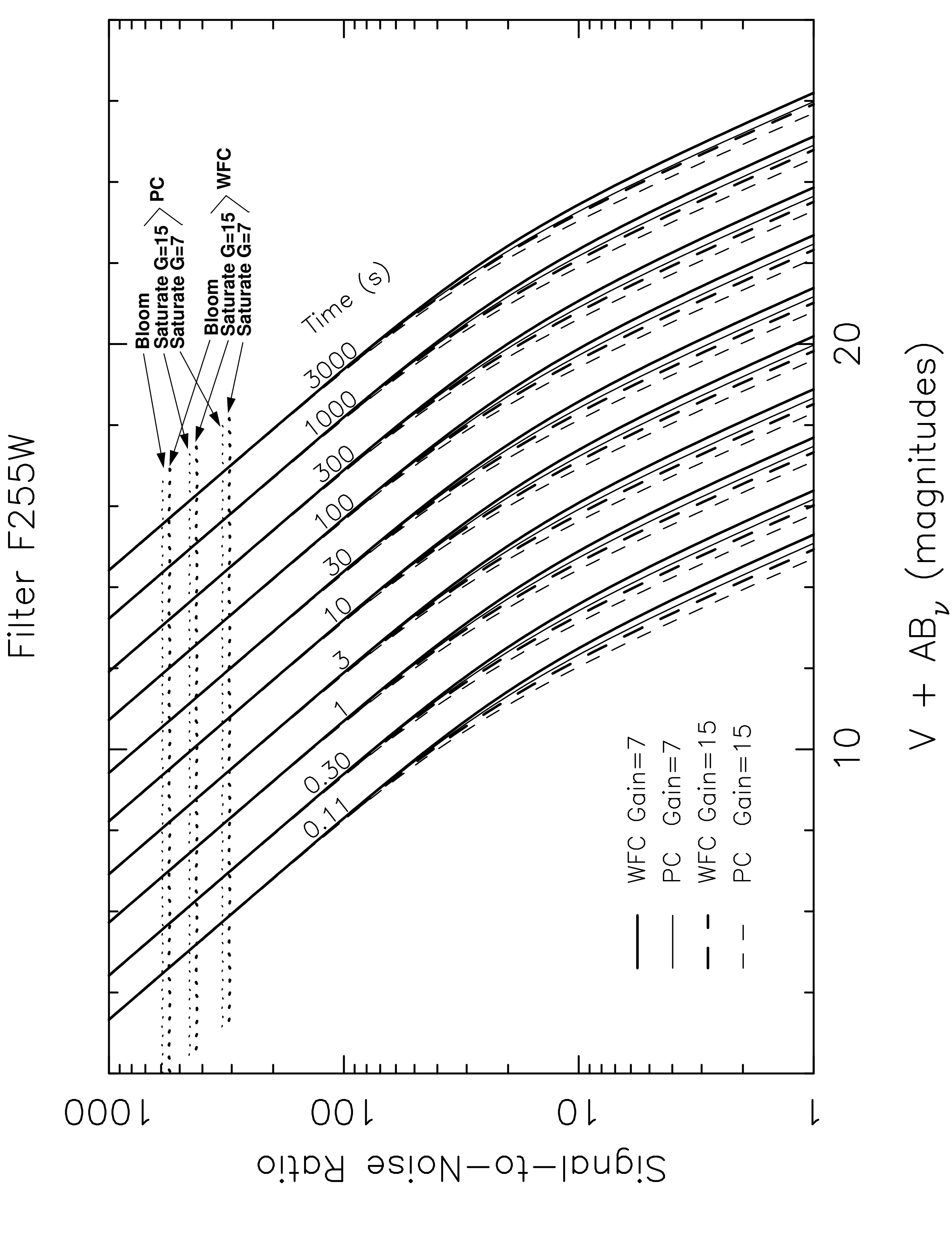

Figure B.4: Point Source SNR vs. V+AB$_\nu$ for F300W Filter.

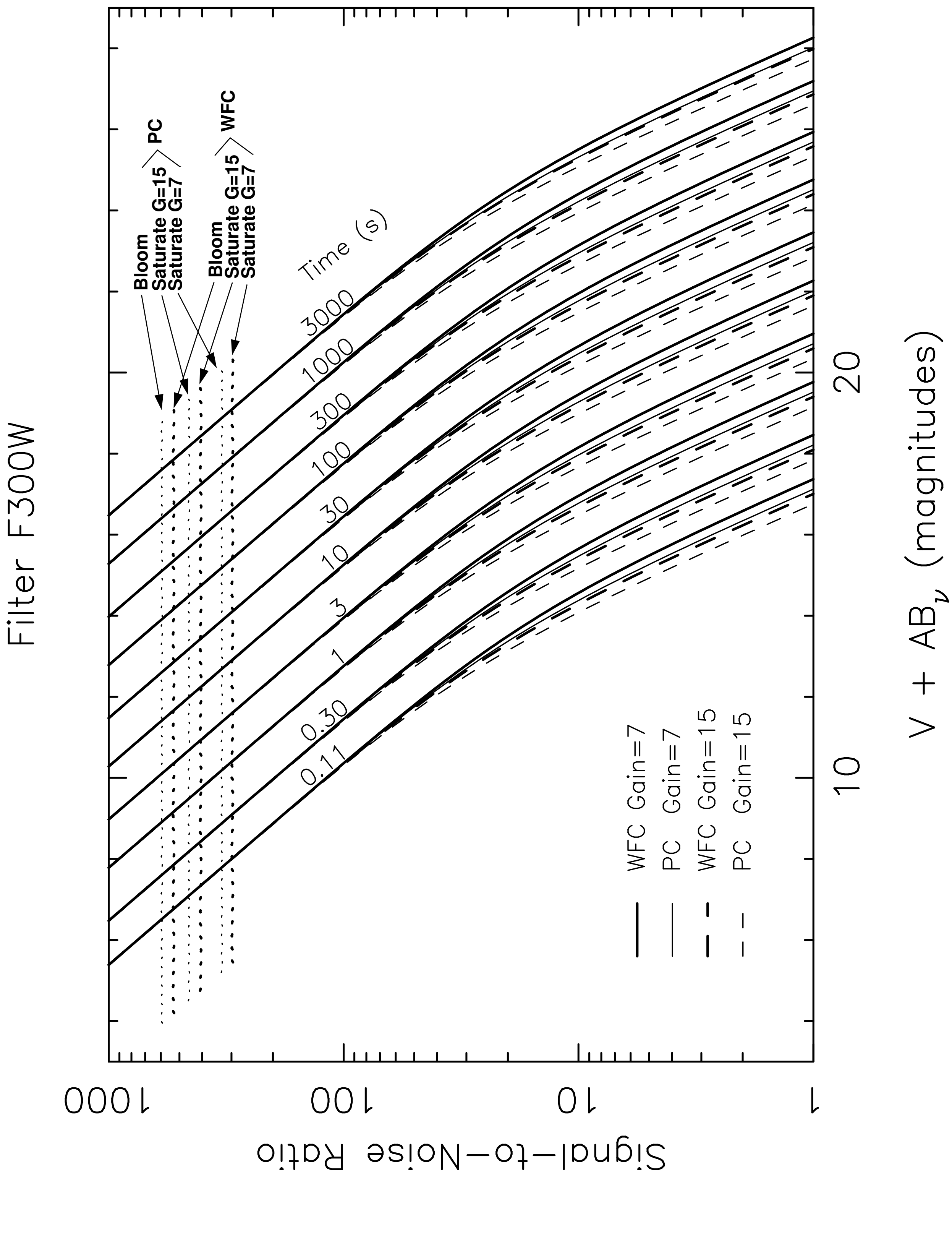

Figure B.5: Point Source SNR vs. V+AB$_{\nu}$ for F336W Filter.

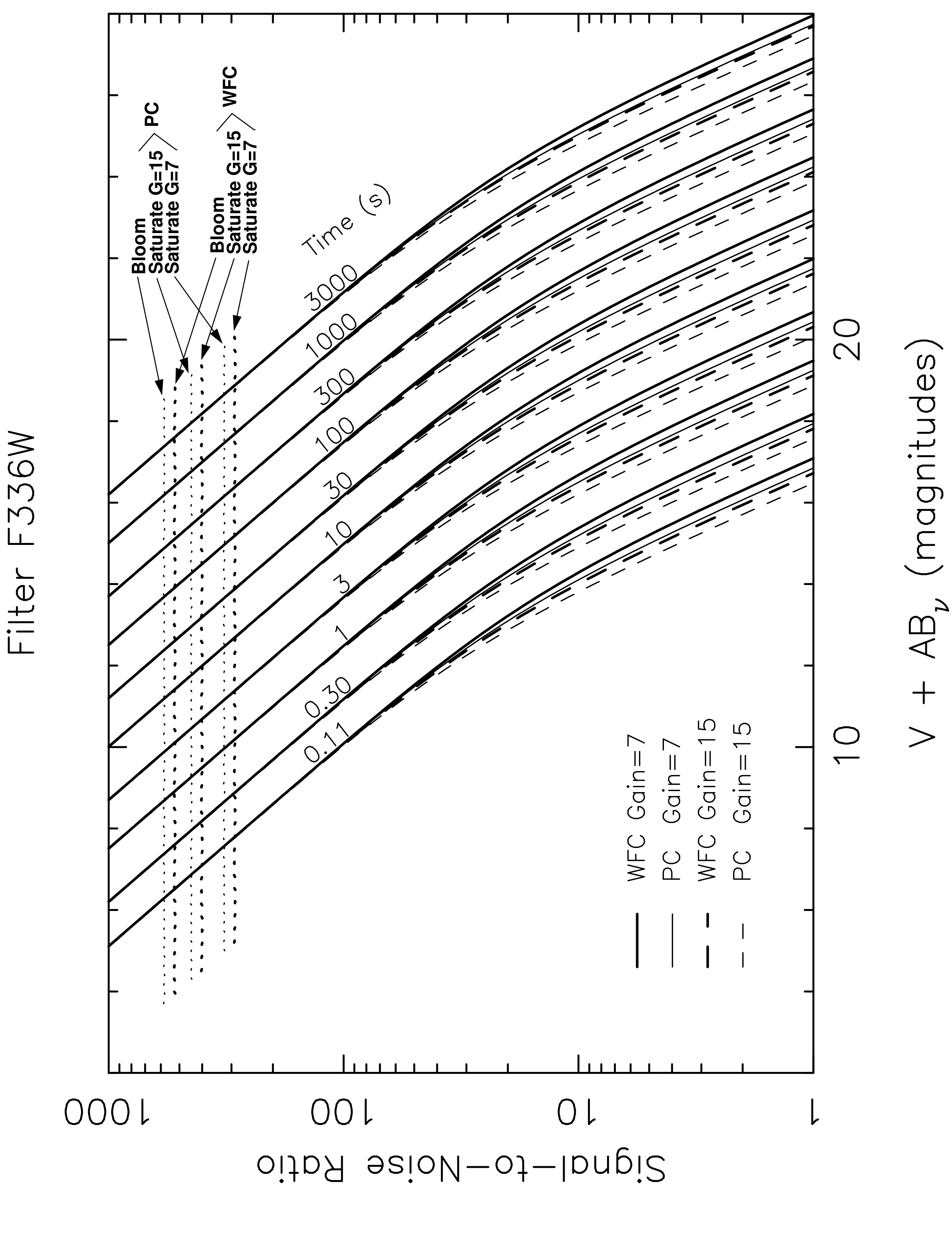

Figure B.6: Point Source SNR vs. V+AB$_\nu$ for F410M Filter.

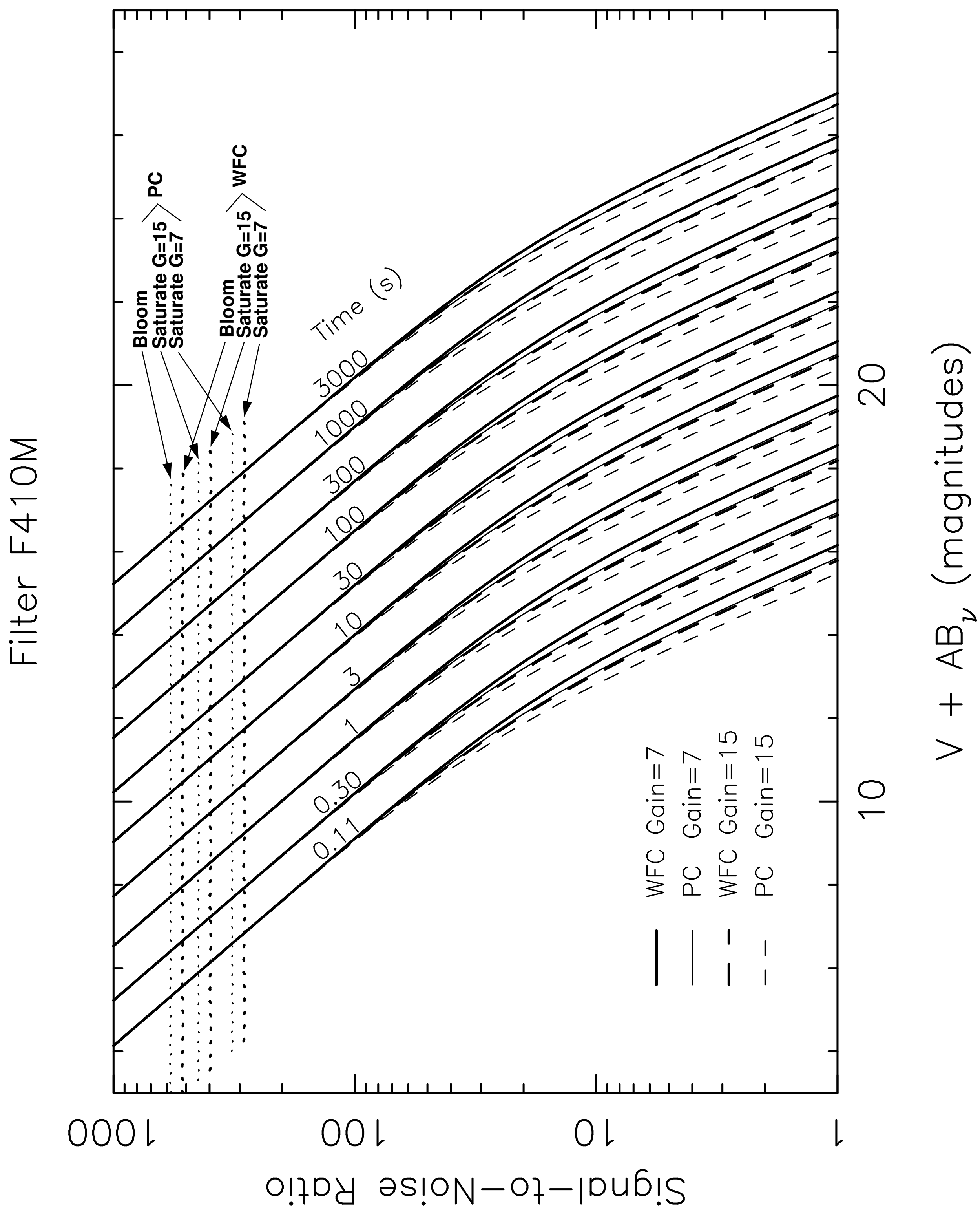

Figure B.7: Point Source SNR vs. V+AB$_\nu$ for F439W Filter.

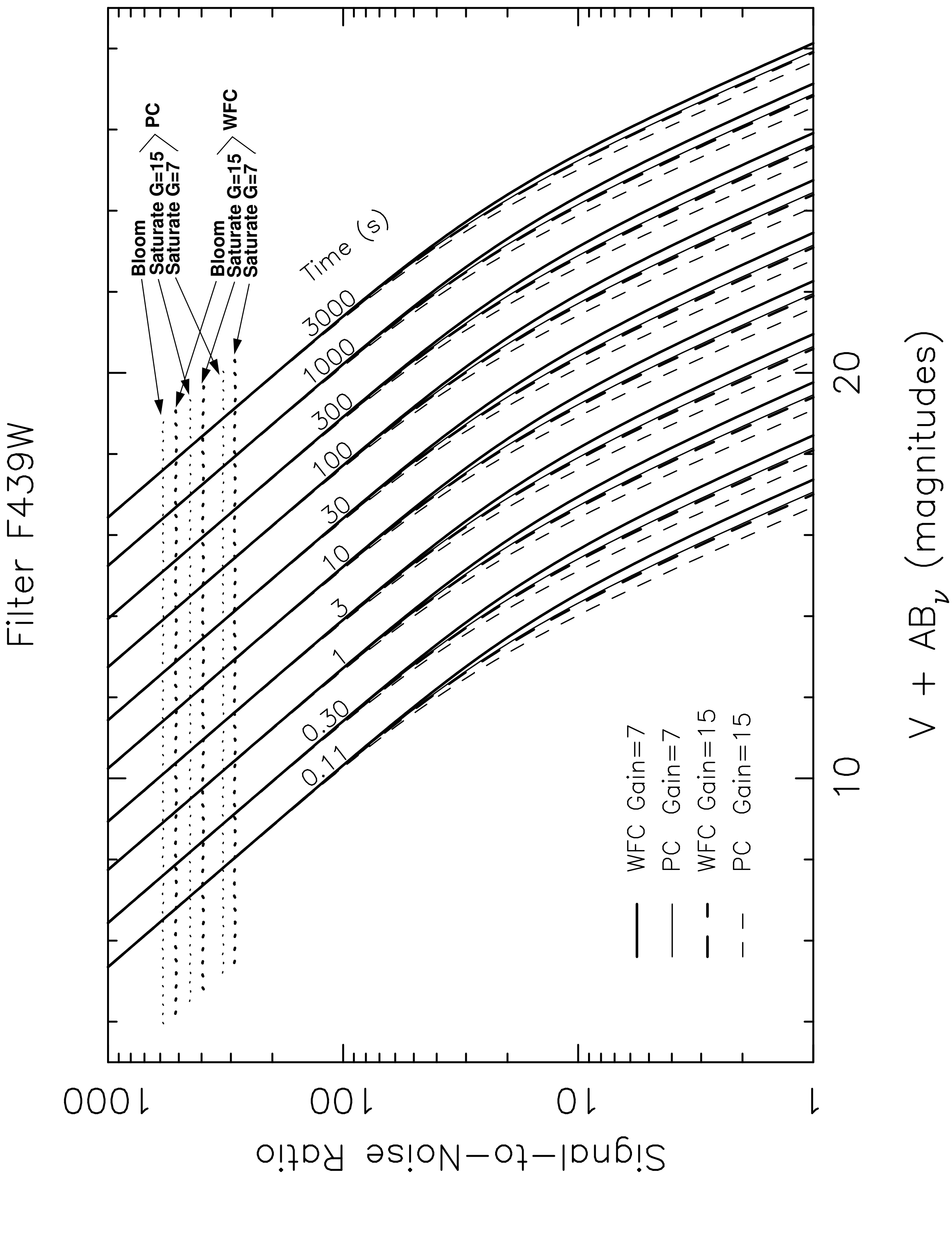

Figure B.8: Point Source SNR vs. V+AB$_\nu$ for F502N Filter.

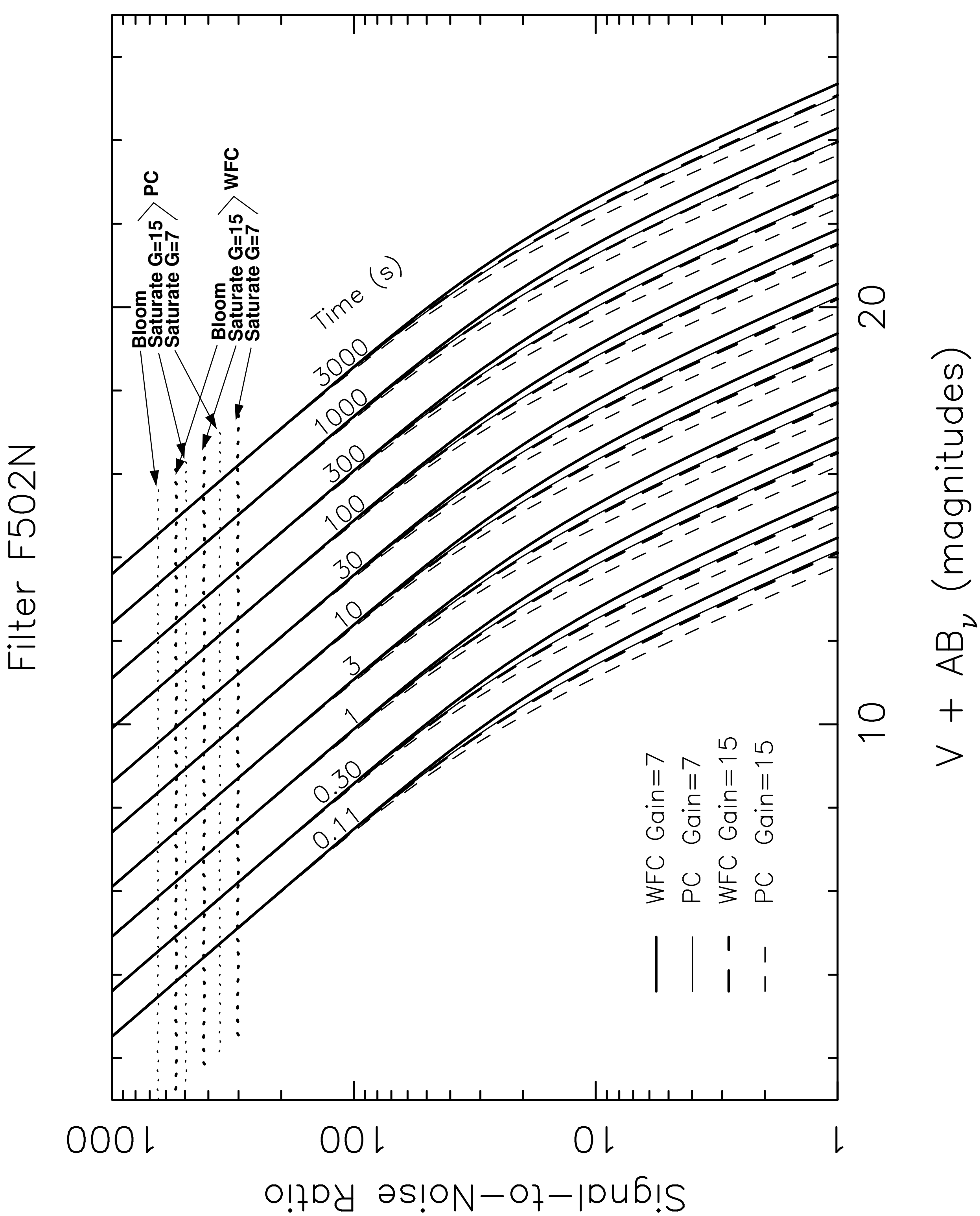

Figure B.9: Point Source SNR vs. V+AB$_{\nu}$ for F547M Filter.

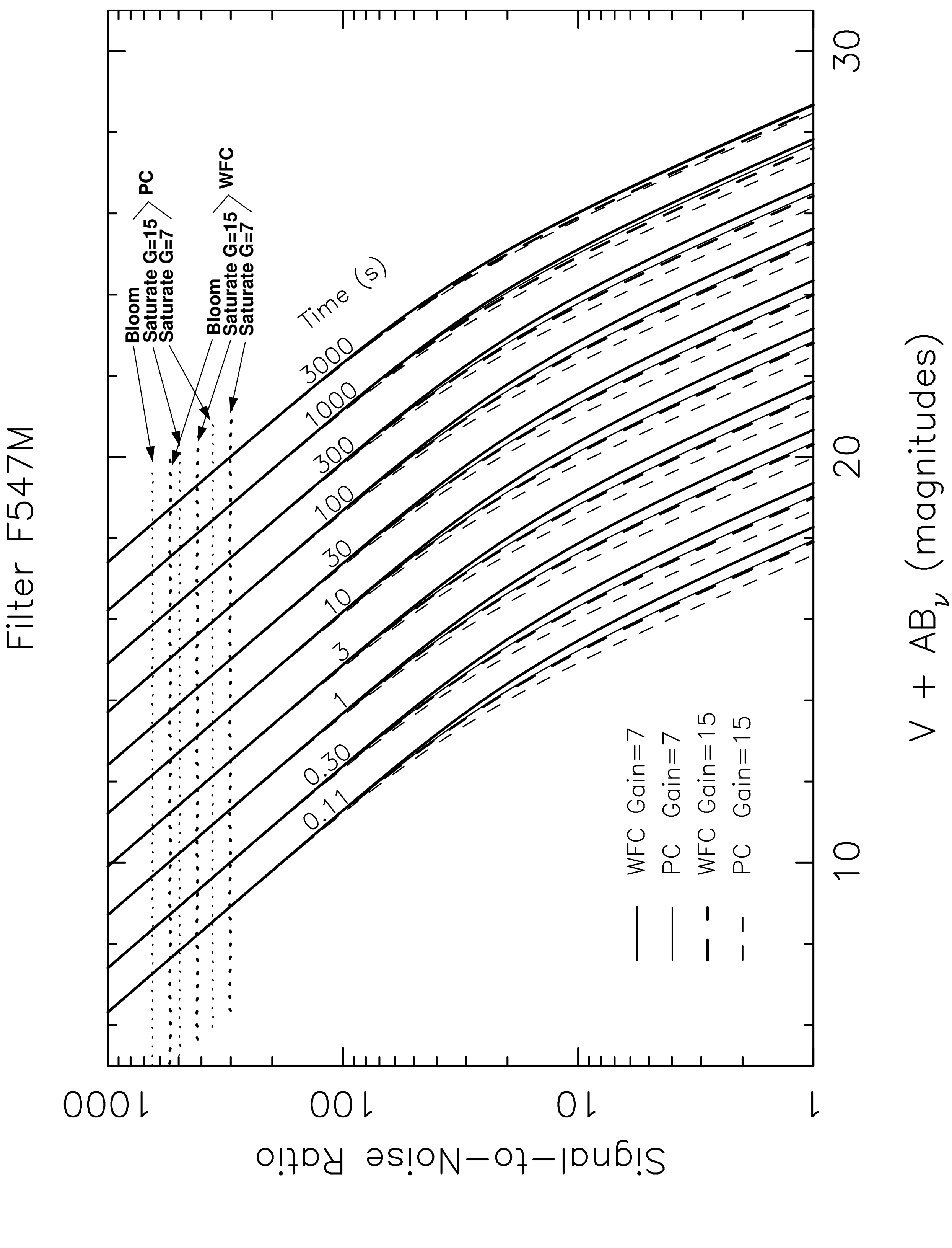

Figure B.10: Point Source SNR vs. V+AB$_\nu$ for F555W Filter.

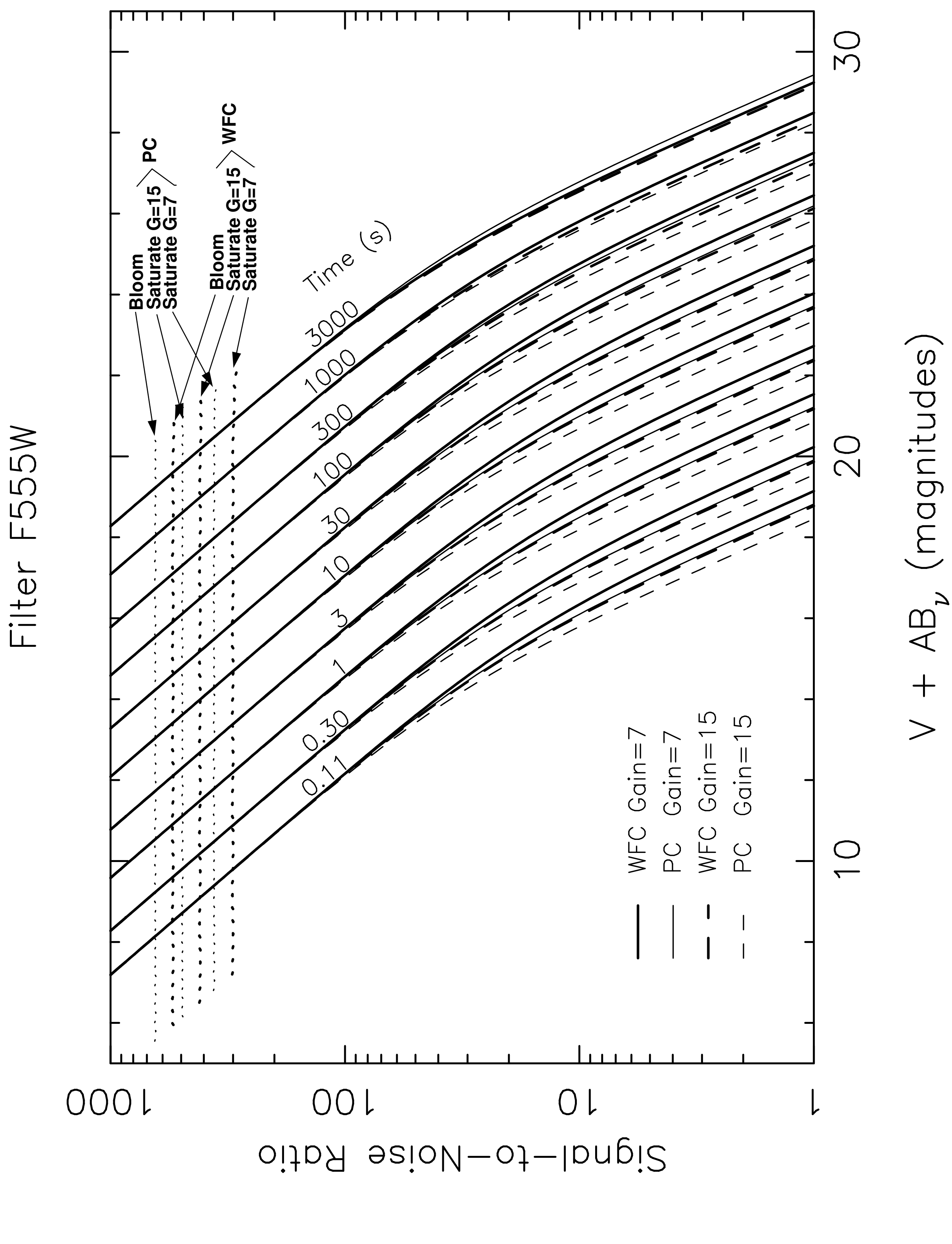

Figure B.11: Point Source SNR vs. V+AB$_\nu$ for F606W Filter.

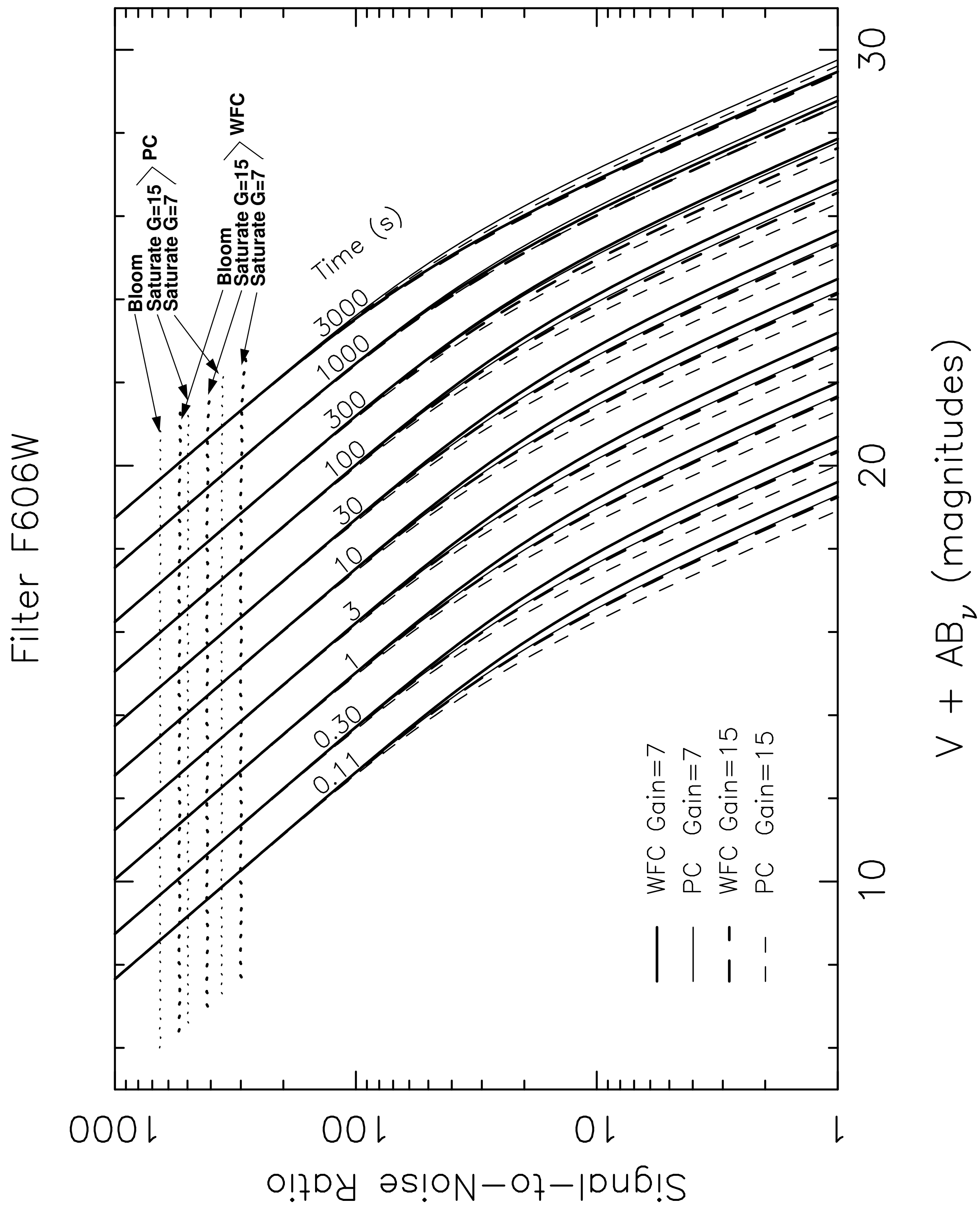

Figure B.12: Point Source SNR vs. V+AB$_\nu$ for F675W Filter.

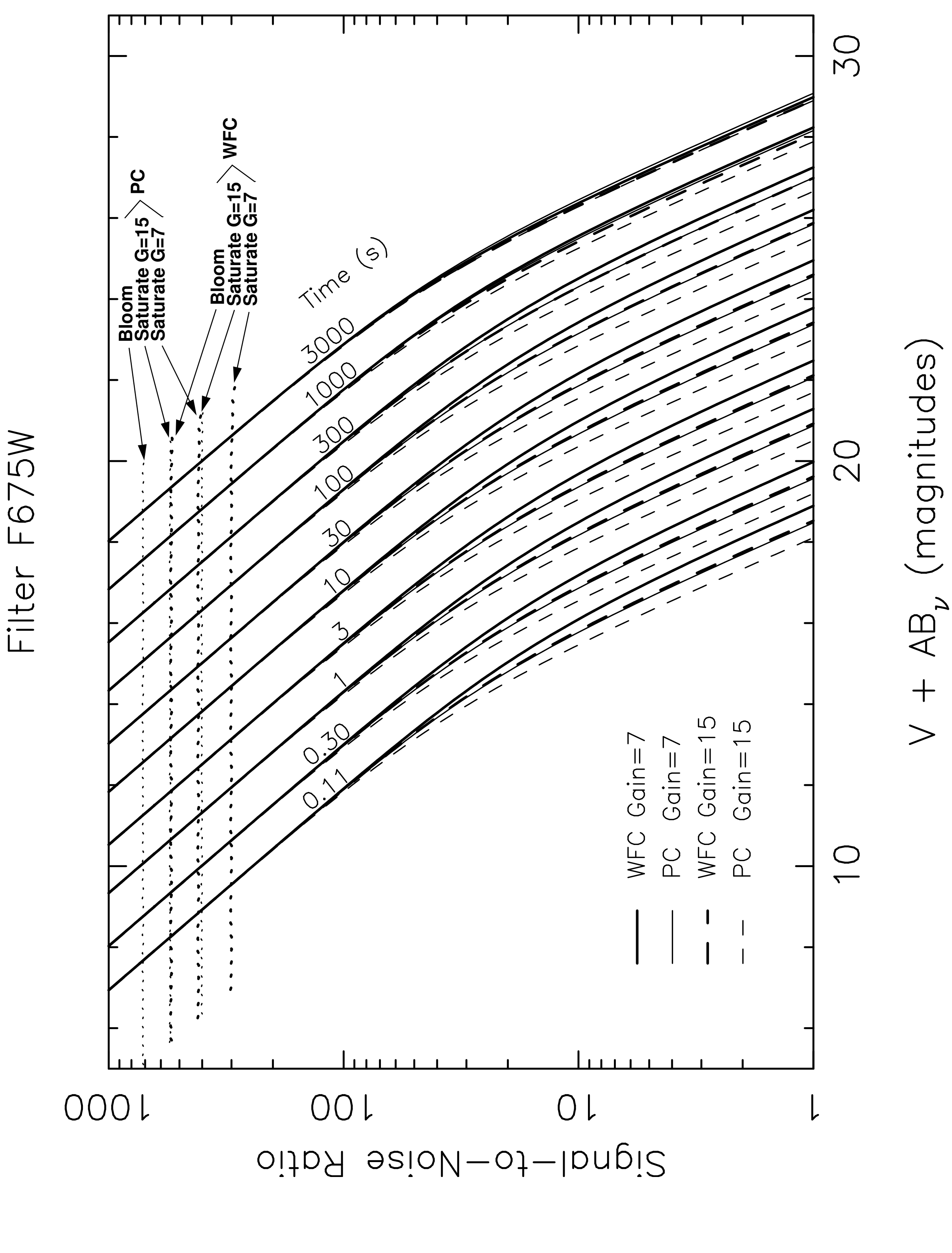

Figure B.13: Point Source SNR vs. V+AB$_\nu$ for F702W Filter.

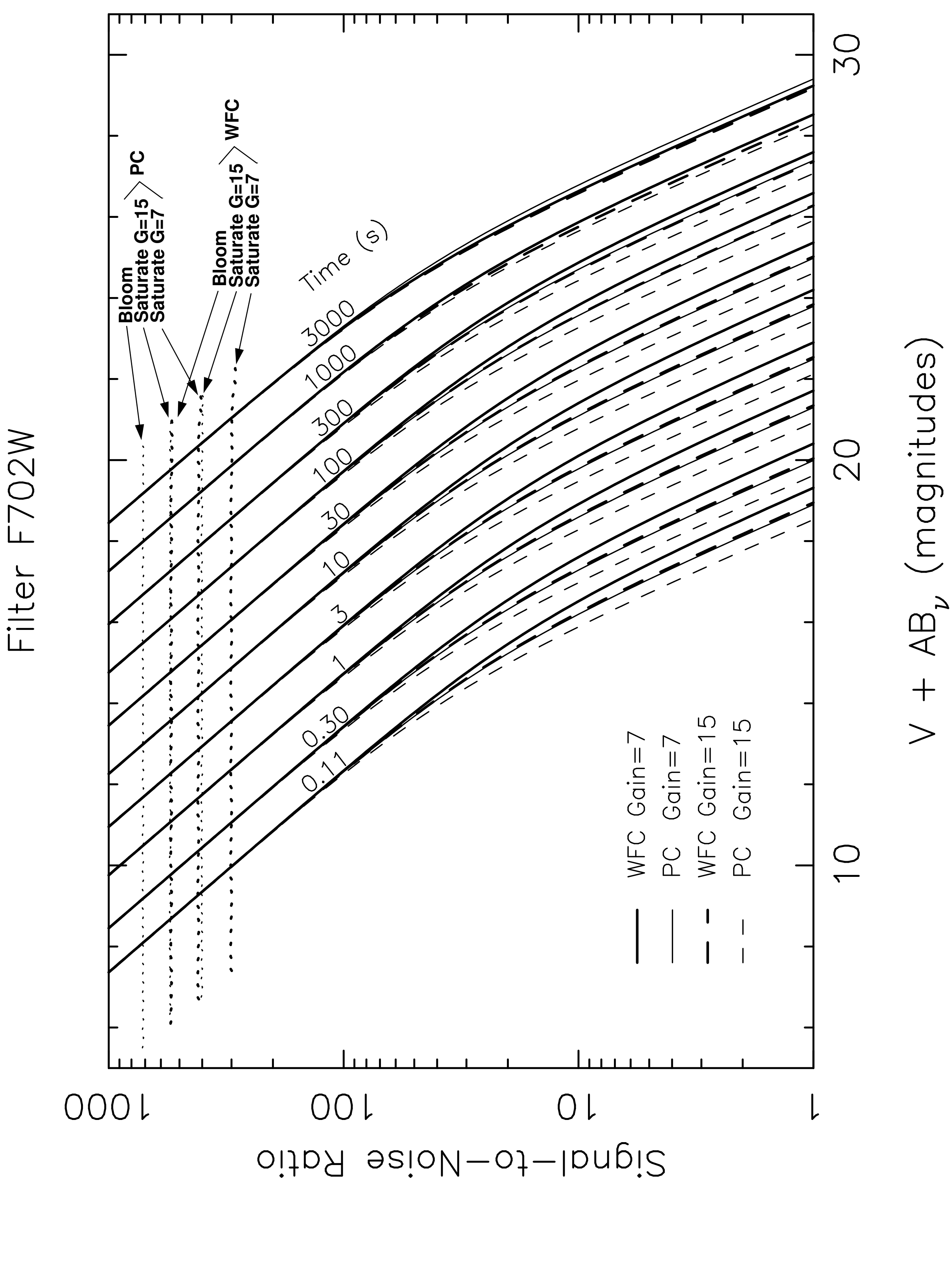

Figure B.14: Point Source SNR vs. V+AB$_\nu$ for F814W Filter.

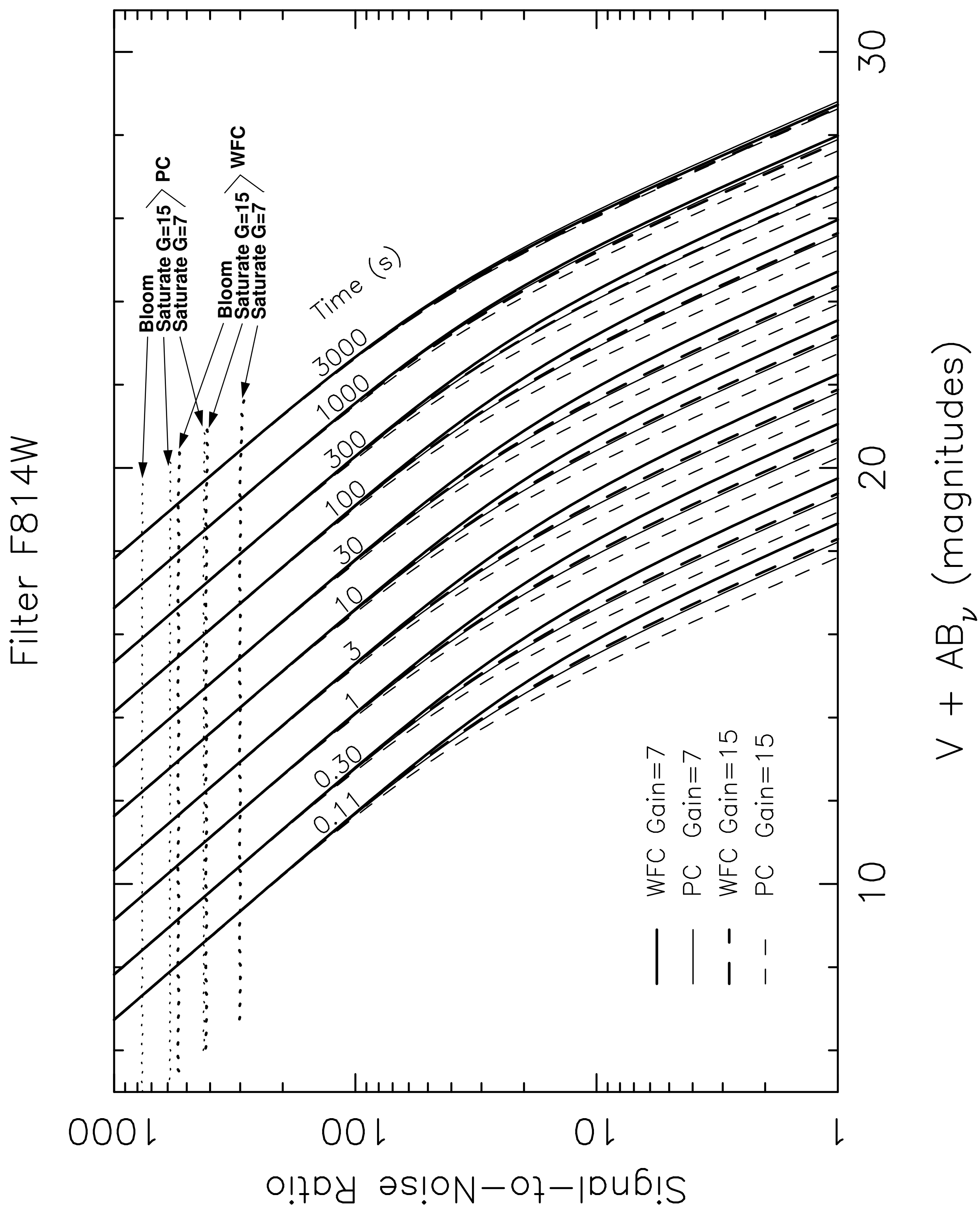

APPENDIX C: Acronyms

Table C.1: Acronyms

ADC	Analog-to-Digital Conversion
ADU	Analog-to-Digital Units (see DN)
CCD	Charge-Coupled Device
CEIS	Contract End Item Specification
CVZ	Continous Viewing Zone
DQE	Detector Quantum Efficiency
DN	Data Number (output of A-to-D converter)
EE	Encircled Energy
FITS	Flexible Image Transport System
FOC	Faint Object Camera
GO	General Observer
GSFC	Goddard Space Flight Center
GTO	Guaranteed-Time Observer
HST	Hubble Space Telescope
ICD	Interface Control Document
IDT	Instrument Definition Team
ISR	Instrument Science Report
JPL	Jet Propulsion Laboratory
LEO	Low Earth Orbit
mas	milliarcsecond
MPP	Multi-Pinned Phase
MTF	Modulation Transfer Function
NICMOS	Near-IR Camera and Multi-Object Spectrograph
OTA	Optical Telescope Assembly
PC	Planetary Camera
PI	Principal Investigator
PODPS	Post Observation Data Processing System
PSF	Point Spread Function
QEH	Quantum Efficiency Hysteresis
RBI	Residual Bulk Image
RMS	Root Mean Square
SLTV	System Level Thermal Vacuum Test

Table C.1: Acronyms

SMOV	Servicing Mission Orbital Verification
SNR	Signal-to-Noise Ratio
STAN	Space Telescope [Data] Analysis Newsletter
STEIS	Space Telescope Electronic Information Service
STIS	Space Telescope Imaging Spectrograph
STScI	Space Telescope Science Institute
STSDAS	Space Telescope Science Data Analysis System
TIPS	Telescope and Instruments Performance Summary
UV	Ultraviolet
WF/PC-1	Wide Field and Planetary Camera
WFC	Wide Field Camera
WFPC2	Wide Field and Planetary Camera 2
WWW	World Wide Web

Index

D

E